



University  
of Glasgow | Department  
of Chemistry

# Research Project Thesis

A novel approach to the total synthesis  
of the piperidine alkaloid (+)- $\alpha$ -  
conhydrine

Iain Alisdair McGeoch  
Supervisor: Dr. Andrew Sutherland

## Abstract

Alkaloids are known for their broad spectrum of pharmacological activity. The piperidine alkaloid conhydrine is an alkaloid for which pharmacological roles have not yet been investigated, although it is known that other alkaloids including the 2-(1-hydroxyalkyl)piperidine motif in conhydrine exhibit important therapeutic activities, e.g. as antiviral or antitumour agents.

A novel approach to the total synthesis of a particular conhydrine diastereomer, (+)- $\alpha$ -conhydrine, will be examined. The synthetic strategy chosen will proceed *via* two key transformations: an ether-directed, palladium(II)-catalysed aza-Claisen rearrangement as the source of stereoselectivity, and a ring-closing metathesis that will form the piperidine core of the target molecule.

The confirmation of the validity of the methodology employed in the synthesis of (+)- $\alpha$ -conhydrine could lead into the application of the same methodology to the synthesis of other natural products or bioactive molecules exhibiting similar structural patterns to that of conhydrine.

## **Acknowledgements**

I would like to thank Dr. Andrew Sutherland for giving me the chance of undertaking a challenging project within his research group. Furthermore, his day-to-day guidance and his full attention on problems I encountered during the course of the project were invaluable. Equally important was the faultless project supervision of Andrew Jamieson, an excellent person and a professional in every single aspect. I have learnt much more than I expected from the project, both at a practical and theoretical level. Finally, I would also like to thank the rest of the Henderson laboratory group for its help and for creating a great environment to work in.

## **Index**

Abstract	1
Acknowledgements	2
Index	3
1. Introduction	
1.1 Background to Alkaloids	4
1.2 Piperidine Alkaloids	6
1.3 Project: A Novel Approach To The Total Synthesis Of The Piperidine Alkaloid (+)- $\alpha$ -Conhydrine	11
2. Results & Discussion	16
Conclusion	40
3. Experimental	41
4. References	47
Appendix	49

# 1. Introduction

## 1.1. Background to Alkaloids

Alkaloids are one of the most important groups of natural products, i.e. compounds that are synthesised by the secondary metabolism of living organisms. These molecules play important roles in the species that synthesise them but are not essential for life, unlike products of primary metabolism, e.g. nucleosides, amino acids, carbohydrates or lipids.<sup>1,2</sup>

Although rare in mammals, alkaloids are particularly abundant in higher plants, insects, amphibians and fungi. Within these species, alkaloids are synthesised to act as poisons or anaesthetics for predators, or even as mediators of ecological interactions. In any case, their purpose is to increase chances of survival.

Generally, alkaloids can be isolated from the species mentioned above or synthesised by organic chemists in the laboratory and then studied as therapeutic agents thanks to their interesting pharmacological properties. Good examples of therapeutic natural product agents are alkaloid analgesics, enzyme inhibitors, tumour suppressants, antibacterials, antiparasitics (antimalarials), antispasmodics, and treatments against hypertension and mental disease.

The name “alkaloid” traces back to 1819 when the apothecary Meissner observed that some plants such as the deadly nightshade, from which the toxic atropine (below) is obtained, could be treated with aqueous acid to give precipitates on neutralisation. Therefore, the plant extracts acted as alkali and were described as alkaloids. The molecular nature of this observation lies in the presence of basic amino groups in these molecules, e.g. in cocaine (Figure 1). The same reasoning applies to their nomenclature, all alkaloids ending in -ine or -in (from amine).

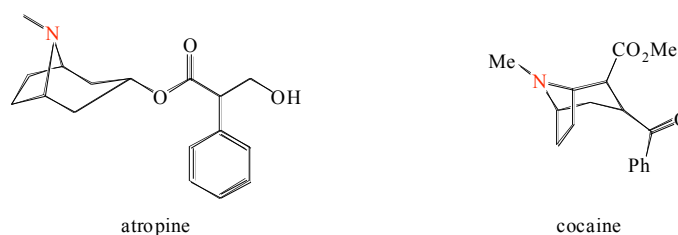


**Figure 1.** Atropine (left), a toxin found in *Atropa belladonna* “the deadly nightshade”, and the tropane cocaine (right), a topical anesthetic isolated from the leaves of *Erythroxylum coca* in south America. The basic amino group of these alkaloids is highlighted in red.

Alkaloids occur mainly as carboxylic acid salts of their nitrogen heterocycles, e.g. citric, lactic, oxalic, acetic, maleic or tartaric acid salts as well as fumaric, benzoic, aconitic and vertaric acid salts. Thus, just as some plants are noted for containing certain alkaloids, they may be equally noted for containing high levels of the particular acid that forms a salt with the alkaloid. However, because of the polar, basic nature of alkaloids, most of these occur dissolved in plant saps as cations, and it is on evaporation of the sap that the organic acid is formed.<sup>3</sup>

Physically, most alkaloids are colourless, crystalline solids slightly soluble in neutral or alkaline aqueous solution but readily soluble in acid or in organic solvents such as ether, chloroform, or ethanol. A few alkaloids (e.g. nicotine and coniine) are liquid at room temperature, and some (e.g. sanguinarine) are coloured (Figure 2).

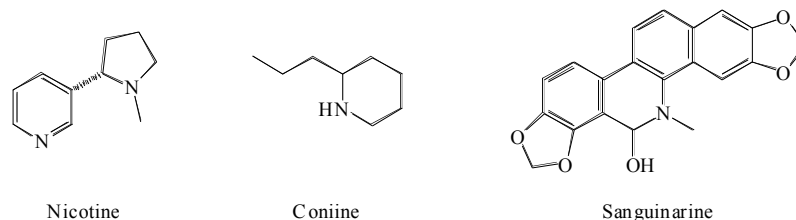


**Figure 2**

Alkaloids derive from amino acids or closely related molecules, and from an evolutionary point of view, they are said to have arisen as biologically active metabolic degradation products of excess amino acids (or amino acid intermediates).<sup>1,2</sup> Thus, alkaloids are classified into different groups based on their carbon-nitrogen skeleton, which is ultimately related to their respective progenitor amino acid:

Benzylisoquinoline alkaloids derive from the amino acid tyrosine, and as their name indicates, they have a benzyl group attached at the 2-position of an isoquinoline ring. Most benzylisoquinolines are derived from two molecules of tyrosine, e.g. papaverin (below). However, not all tyrosine-derived alkaloids are benzylisoquinolines, e.g. nescaline. It is the  $ArC_2N$  unit in these alkaloids that identifies their progenitor amino acid (Figure 3).

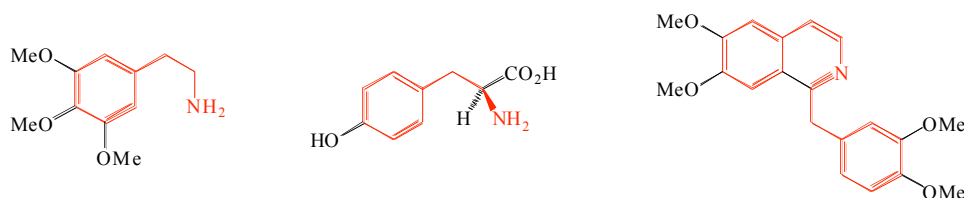


**Figure 3.** Mescaline (left) and papaverin (right) are benzylisoquinoline alkaloids derived from the amino acid tyrosine (centre). The diagnostic  $ArC_2N$  core of these molecules is highlighted in red.

Tryptophan derived alkaloids are usually clearly distinguishable by their indole skeleton, e.g. the hallucinogen psilocin, or the ergot alkaloids lysergic acid diethylamide (LSD), also a hallucinogenic agent (Figure 4). Ergot alkaloids are a subclass of tryptophan-derived alkaloids, they are synthesised from lysergic acid, which in turn is synthesised from tryptophan.



**Figure 4.** Psilocin (left) and LSD (right) are alkaloids derived from tryptophan (centre). The clearly discernible indole/tryptophan motif is highlighted in red.

Piperidine and pyrrolidine alkaloids form one of the largest groups of alkaloids known, and as their name indicates, they include a piperidine or pyrrolidine core in their structures, which are derived from the amino acids lysine and ornithine respectively (Figure 5). These two core structures differ only in the length of their carbon-nitrogen skeleton, piperidines being six membered- and pyrrolidines being five membered rings. Ignoring the one-carbon difference in length, the biosynthesis of these units is identical, and therefore the report will focus on piperidine alkaloids only, as they will be the main theme throughout the proposed project.

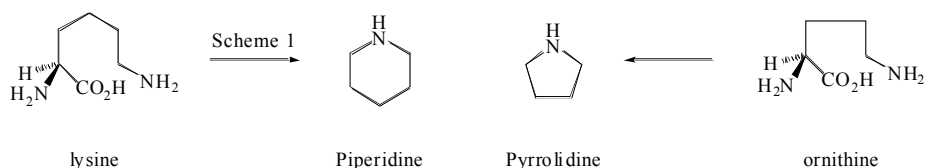
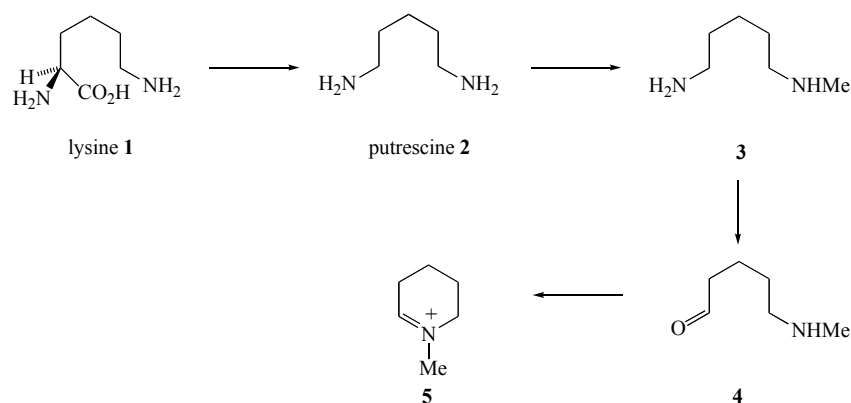


**Figure 5.** The piperidine and pyrrolidine units are derived from lysine and ornithine respectively in nature.

## 1.2. Piperidine Alkaloids

### 1.2.1. Biosynthesis

The biosynthesis of the piperidine unit (or its reactive iminium equivalent to be specific) from lysine is shown below (Scheme 1). Lysine **1** is decarboxylated (a) to give the symmetrical diamine putrescine **2**, which is then methylated (b) to form the asymmetrical diamine **3**, and transaminated (c) to give **4**. The amine and carbonyl groups in **4** can undergo intramolecular condensation (d) to form the iminium ion **5**, which can undergo a wide range of reactions such as nucleophilic attack at the 2-position to form an equally broad variety of piperidine alkaloids (Figure 6).<sup>1,2</sup>



**Scheme 1.** Lysine undergoes a sequence of *in vivo* enzyme-catalysed reactions to give the reactive piperidine iminium ion (5). Evidence for this biosynthetic pathway comes from  $^{14}\text{C}$  radiolabelling studies.

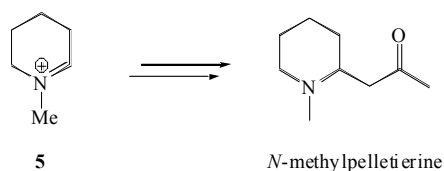


**Figure 6.** The piperidine core unit is further modified by a range of enzymatic reactions to give the final piperidine alkaloid. In the example shown, the quaternary iminium species reacts with acetoacetate to give the piperidine alkaloid *N*-methylpelletierine.

Most of these processes are catalysed by enzymes in the body, a good example being the transamination step (c) in Scheme 1, which is pyridoxal phosphate-catalysed. Most importantly, many alkaloids are optically active, and the fact that they rarely occur as racemic mixtures is taken as evidence that they are synthesised at least partially by enzymatic catalysis. In some cases enantiomorphs are known to be naturally occurring, but each from a different source.<sup>3</sup>

It is therefore a major challenge for synthetic chemists to emulate all these biological reactions in the laboratory and to develop efficient and stereoselective methodologies for the synthesis of natural products. However, it is realistic to state that the main driving force in the synthetic interest in alkaloids is the broad therapeutic potential of these compounds.

### 1.2.2. Classification & Pharmacology

The piperidine ring is one of the most common structural features found in biologically active agents.<sup>4,5</sup> Watson *et al* established that thousands of piperidine compounds were included in clinical and pre-clinical trials over a recent ten year period.<sup>6</sup> It is therefore convenient to arrange this large family of compounds into different subclasses based on the varying structural patterns amongst them.<sup>7</sup>

1) *N*-acyl derivatives of piperidine

The first alkaloid of this series, *N*-piperyl piperidine or piperine (Figure 7), was discovered in 1938 and since then many other *N*-acyl derivatives have been isolated, many of these open-chain polyalkenoic and acetylenic *N*-acyl derivatives.

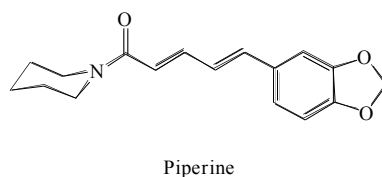


**Figure 7.** Piperine, a piperidine alkaloid isolated from black pepper in 11% yield.

Many *N*-acyl or “piper” alkaloids (including piperine itself) possess antimicrobial activity, as well as being effective in the treatment of asthma and chronic bronchitis.<sup>8</sup> These alkaloids are often included in the formulation of drug prescriptions in India, as they are believed to increase the bioavailability of the drugs with which they are combined. A specific example is the increase of the anti-arrhythmia drug sparteine blood levels by 100% when dosed in the presence of piperine.

During the last two decades, the action of piperine upon the central nervous system (CNS) has been unveiled.<sup>9</sup> It has been shown that this alkaloid possesses anticonvulsant properties in rodents and that it can act as an antiepileptic agent in man. A close derivative of piperine, antiepilepsinine, is commonly employed in China in the prevention of epileptic attacks since 1975.

However, *N*-acyl piperidines in general show behaviour similar to that of classic CNS depressants, only differing in the fact that high doses of *N*-acyl piperidine alkaloid do not lead to anaesthesia.

## 2) Alkyl piperidines

Coniine and coniceines, e.g.  $\gamma$ -coniceine, are the most cited examples of alkyl-piperidines (Figure 8). These two highly toxic alkyl piperidine alkaloids co-occur in the hemlock, the poisonous nature of which has been known for many centuries – indeed it was an extract of this plant that was used to cause the death of Socrates around 400 B.C.<sup>7</sup>

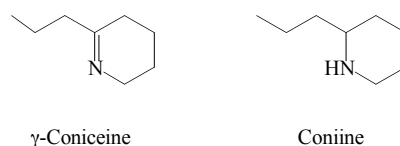


**Figure 8.** Deadly neurotoxic alkyl-piperidines.

The pharmacological properties of coniine have been largely studied for many years. This alkaloid shows neuromuscular blocking effects and it is believed it is the source of the sedative, narcotic, anodyne, antispasmodic and anaphrodisiac properties of the

poison hemlock.<sup>10,11</sup>  $\gamma$ -coniceine shows almost identical pharmacological activity to that of coniine, however it is six times as potent but occurs in much smaller concentrations in the poison hemlock.<sup>12</sup>

### 3) Piperidine alcohol and ketone alkaloids

A convenient example of a piperidine alcohol is the 2-(1-hydroxyalkyl)piperidine conhydrine, yet another alkaloid of the poison hemlock.<sup>7</sup> This natural product will be revisited in more detail at a later stage, as it is the target molecule of the synthetic pathway proposed for the project.

Conhydrinone, the product of oxidation of conhydrine, has also been known for a long time, however it was not until recently that it was isolated from the poison hemlock (Figure 9).<sup>13</sup>

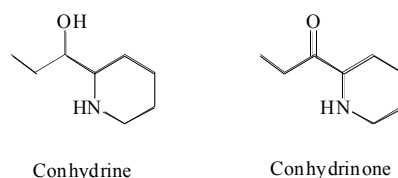


**Figure 9.** Conhydrine and its product of oxidation, conhydrinone.

2-(2-hydroxyalkyl)piperidines are also known. Sedridine (Figure 10) co-occurs with other 2-(2-hydroxyalkyl)piperidines in the plant *Sedum Acre*.<sup>14</sup>

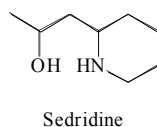


**Figure 10**

Little is known about the pharmacology of these compounds. However, bearing in mind that most alkaloids have a biological role that can be exploited from a therapeutic point of view, the lack of pharmacological knowledge on these natural products makes them a highly interesting synthetic target.

The best studied alkaloids in this subclass of piperidines are pelleterines, a series of piperidine ketones which are widely employed as effective anthelmintic agents.<sup>15</sup> *N*-methylpelleterine (Figure 6) acts locally within the gastrointestinal tract to eradicate tapeworms, although it is also related to the side effects observed, e.g. muscle cramps and convulsions.

### 4) Piperidine alkaloids with long aliphatic sidechains

This sort of piperidine alkaloid is very common in the animal kingdom, especially in insects, although it is also found in plants.<sup>7</sup> An example of these alkaloids is solenopsin A, isolated as a large constituent of the venom of fire ants (Figure 11).<sup>16</sup> Solenopsin A and closely related piperidines with long alkyl or alkenyl sidechains have recently been shown to effectively inhibit  $\text{Na}^+/\text{K}^+$ -ATPase activity in the brain.

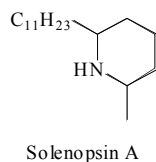


**Figure 11.** Solenopsin A, an ATPase inhibitor present in the venom of fire ants.

### 5) Other piperidine alkaloids

Fused ring piperidines and spiro-piperidines are also found in nature and comprise a broad spectrum of pharmacological activity. An example of a spiro-piperidine is histrionicotoxin, a local anaesthetic isolated from the Colombian frog. A representative fused-ring piperidine example is adaline, which includes an azabicyclononane skeleton and is a defensive alkaloid present in the European ladybug *Adalia Bipunctata* (Figure 12).<sup>7</sup>

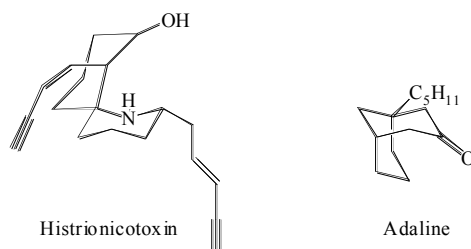


**Figure 12**

It is important not to confuse fused-ring piperidine alkaloids with tropanes, which include a fused piperidine-pyrrolidine ring system. The biosynthesis of tropanes such as cocaine (see Figure 1) is believed to proceed via an ornithine-derived pathway typical of pyrrolidine alkaloids and not *via* the lysine pathway illustrated in Scheme 1. The remaining four carbons of the cocaine fused-ring skeleton are derived from two successive additions of acetate.<sup>1</sup>

### 1.2.3. Synthesis of Piperidine Alkaloids

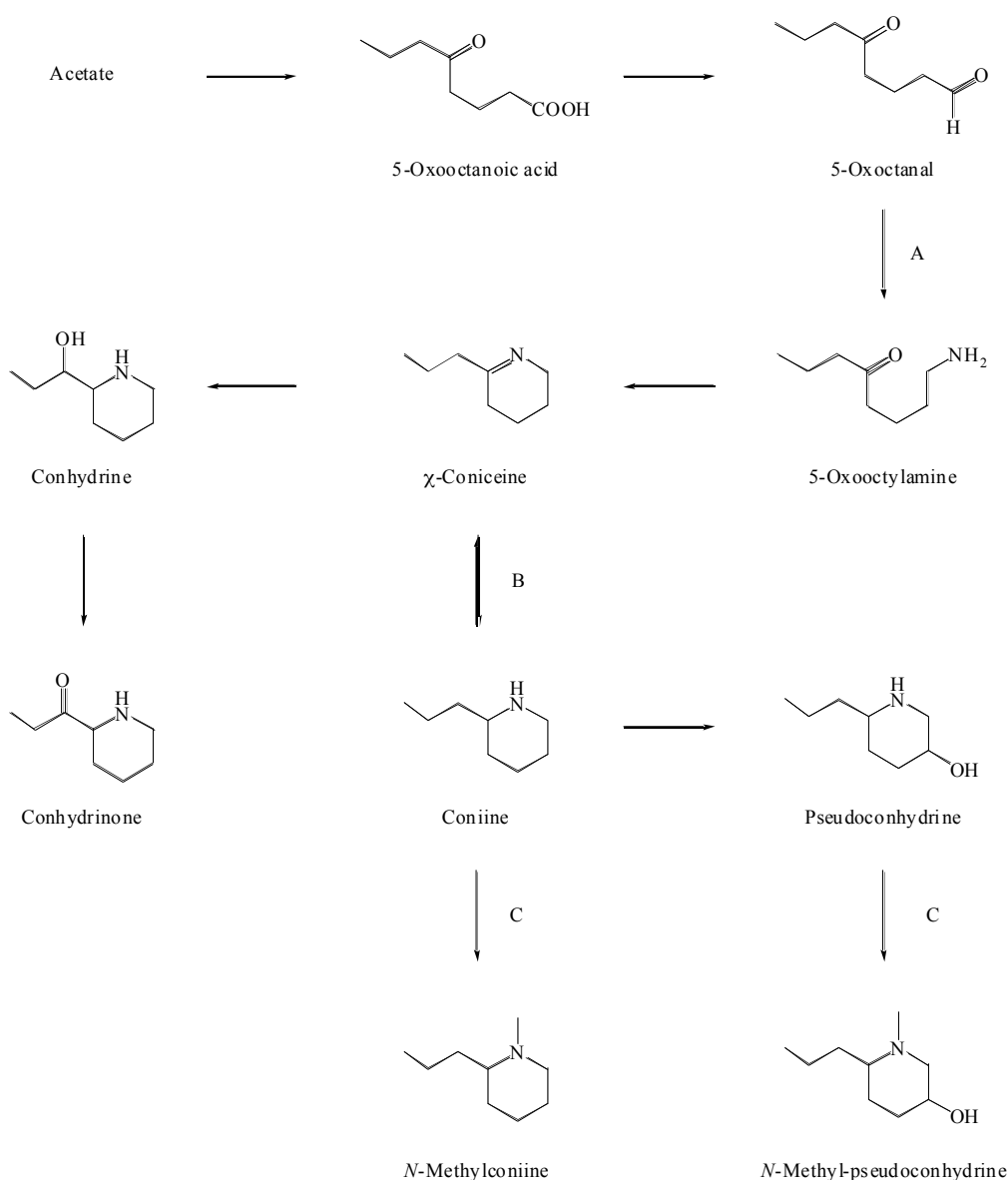
The chemical synthesis of piperidine alkaloids was largely reviewed in the introduction essay to the project and will not be revisited in this thesis. Common synthetic methodologies employed in the synthesis of piperidine compounds include nucleophilic substitutions, reductive aminations, Michael additions, diene chemistry (mainly ring-closing metathesis), cycloadditions, and reductions of pyridones, lactams, tetra- and dihydropyridines.

### 1.3. Project: A Novel Approach To The Total Synthesis Of The Piperidine Alkaloid (+)- $\alpha$ -Conhydrine

There are two distinct yet related sides to the proposed project. One can adopt a chemical approach for which the interest lies in the methodology and the synthetic route employed in the synthesis of the piperidine alkaloid, or one can focus on the importance of the actual target alkaloid and that of other related potential targets. In any case, both approaches are closely related and both will be considered, although due to the fact that the practical work of the project was purely chemical in nature, emphasis will be laid on the chemistry.

#### 1.3.1 Biochemistry underlying project

The aim of the project is in the synthesis of the 2-(1-hydroxyalkyl)piperidine alkaloid conhydrine. Conhydrine is isolated from the poison hemlock *Conium Maculatum* and is present in relatively small concentrations.<sup>17</sup> The alkaloid co-occurs in the plant with the alkyl piperidines coniine, *N*-methylconiine and  $\gamma$ -coniceine, with the piperidine alcohols pseudoconhydrine and *N*-methylpseudoconhydrine, and with the piperidine ketone conhydrinone. The postulated biosynthesis of these alkaloids in the poison hemlock is depicted below (Scheme 2).



**Scheme 2.** The biosynthesis of poison hemlock alkaloids. The postulated pathway involves a linear arrangement of four acetate units. Well-defined enzymatic transformations: transamination with *L*-alanine catalysed by 5-oxooctanal-aminotransferase (A), an NADPH-dependent and reversible  $\chi$ -coniceine reductase-catalysed reduction (B), and *S*-adenosyl-*L*-methionine-methyltransferase-catalysed methylations (C).

Conhydrine was discovered in the poison hemlock in 1856 and was then assigned its correct empirical formula:  $C_8H_{16}ON$ .<sup>18</sup> It is a solid crystallizing as colourless leaflets from ether (m.p.  $120.6^\circ C$ , b.p.  $224-5^\circ C / 720\text{ mm}$ ), and is soluble in ethanol or chloroform but only moderately so in water and ether.<sup>19</sup>

When conhydrine is treated with a dehydrating agent, it loses water and a mixture of coniceines is obtained, the content of which depends on the dehydrating agent employed.<sup>20</sup>

Conhydrine can occur in four different diastereomeric forms (Figure 13), one of which will be pursued as the synthetic target of the project (see later).

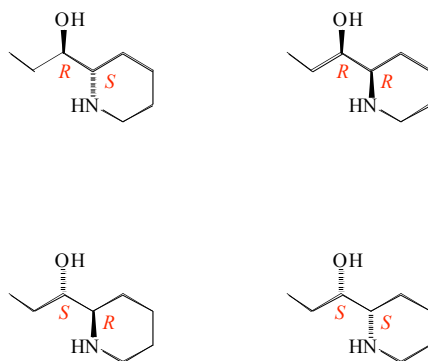
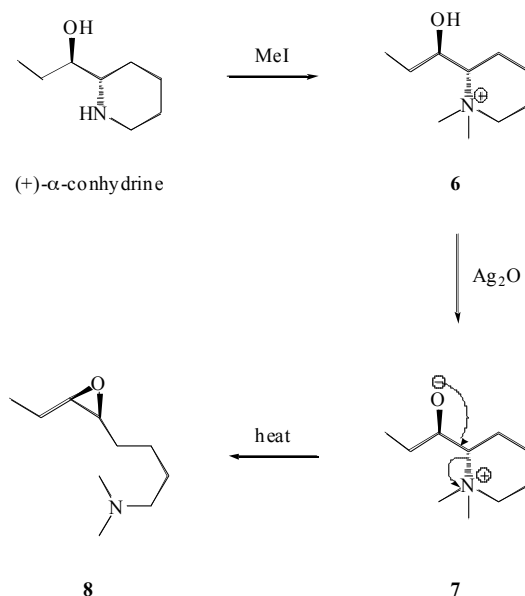


**Figure 13.** Conhydrine can occur in four different diastereomeric forms due to the presence of two chiral centres in the molecule.

The structure of conhydrine has been chemically established with the help of Hoffman degradation studies.<sup>21</sup> The presence of a quaternary nitrogen atom with a hydroxyl group at the  $\beta$ -position enables the elimination of the quaternary centre under basic Hoffman conditions with the formation of an epoxide (Scheme 3). Additional structural studies have verified the structure of conhydrine, and hydroxy-isomers of this alkaloid have been synthesised and contrasted, showing different properties to those of conhydrine.<sup>22</sup>



**Scheme 3.** Hoffman degradation of conhydrine.

Conhydrine is methylated to give the quaternary ammonium species **6** and the alkoxide anion in **7** is then formed in the presence of  $\text{Ag}_2\text{O}$ . Nucleophilic attack of the alkoxide anion on the  $\alpha$ -centre forms epoxide **8** with elimination of the quaternary centre and opening of the piperidine ring.

The toxicology of conhydrine is well defined, it is a neurotoxin as the alkyl piperidines it co-occurs with but is much less potent, and therefore, its toxicity is usually neglected.<sup>23</sup> On the other hand, no pharmacological/therapeutic role has been assigned to any of its diastereomers.<sup>7</sup>

However, it is known that other alkaloids containing the 2-(1-hydroxyalkyl)piperidine moiety are biologically active, e.g. the indolizidine alkaloids (-)-castanospermine and (-)-swainsonine (Figure 14).<sup>24</sup>

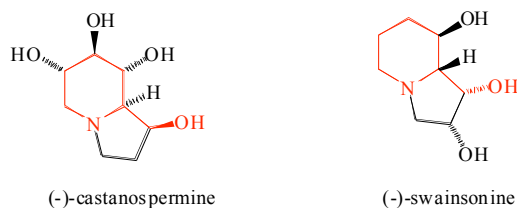


**Figure 14.** The indolizidine alkaloids castanospermine and swainsonine include a 2-(1-hydroxyalkyl)piperidine core, highlighted in red.

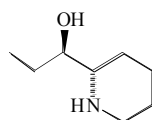
These compounds have been shown to exert potent inhibition of glycoprotein processing, which is directly related to their antiviral activity and possibly to their antitumour properties. Their antiviral action was established with a study in which the influenza virus was raised in the presence of castanospermine, which made the viral glycopeptides liable to the action of endoglucosaminidase, leading to the death of the virus. This was not the case in influenza viruses grown in the absence of the alkaloid.

The pharmacological role of these indolizidine compounds together with the lack of knowledge on conhydrine pharmacology makes the synthesis of conhydrine itself and other compounds incorporating the 2-(1-hydroxyalkyl)piperidine pattern an interesting field.

It is therefore important to possess a reliable and efficient underlying methodology in the syntheses of such compounds. The proposed project will apply established methodologies to the synthesis of (+)- $\alpha$ -conhydrine and will confirm their validity in the general synthesis of compounds including the 2-(1-hydroxyalkyl)piperidine moiety.

### 1.3.2. Chemistry underlying project

The aim of the project is in the synthesis of a natural stereoisomer of conhydrine, (+)- $\alpha$ -conhydrine, where (+) refers to the direction in which the molecule polarises light and  $\alpha$  is the position of the piperidine ring at which the hydroxyalkyl sidechain is located (Figure 15).



(+)- $\alpha$ -conhydrine

**Figure 15**

Due to the availability of starting materials, it was not conhydrine itself but an analogue of it containing a one-carbon shorter alkyl sidechain that would be synthesised. The full synthetic pathway towards this compound is shown below (Scheme 4). The proposed synthesis of (+)- $\alpha$ -conhydrine is based around two key steps: an ether-directed, palladium(II)-catalysed aza-Claisen rearrangement as the crucial stereoselective step, and a ring-closing metathesis (RCM) that will form what will be the piperidine core of the alkaloid. The background to these processes was reviewed in detail in the introduction essay to the project and will only be revisited wherever necessary.

The first stereogenic centre that is to be present in the target molecule is incorporated in the very first substrate of the synthetic route, Methyl-(*R*)-lactate **9**. The hydroxyl group of the lactate was to be protected as the methoxymethyl (MOM) ether and the ester group was then to be reduced to the primary alcohol **10** with the reducing agent DIBAL-H. A one-pot Swern oxidation/Wadsworth-Emmons reaction was to oxidise the alcohol to the aldehyde and was then to form the *E*-allylic ester **11** on reaction with triethylphosphonoacetate. DIBAL-H was again to be employed to reduce the ester to the primary alcohol **12**. The allylic alcohol would then be converted to the key aza-Claisen trichloroacetimidate substrate **13** on reaction with trichloroacetonitrile in the presence of 1,8-diazabicyclo[5.4.0]undecene-7 (DBU). The trichloroacetimidate was to undergo a Palladium(II)-catalysed rearrangement that was to introduce the second stereocentre present in the future (+)- $\alpha$ -conhydrine analogue. The resulting trichloroamide **14** was to be hydrolysed to the amine and then protected with a Boc-group to give amine **15**. Alkylation of this amine with 4-bromo-1-butene was to introduce the second terminal alkene group to yield diene **16**, crucial towards ring closure. RCM with Grubb's catalyst was to give the unsaturated piperidine **17**, which was to be reduced by hydrogenation to yield piperidine **18**. Finally, all protecting groups were to be removed under acidic conditions to afford the analogue of (+)- $\alpha$ -conhydrine **19**.



There are different mechanistic routes *via* which the protection could proceed. The first of these is an S<sub>N</sub>2 process in which the alcohol **9** acts as the nucleophile displacing the bromide anion from Bromomethyl-methyl ether (MOMBr) **21** to give the MOM-protected ether **20**. (Figure 16).

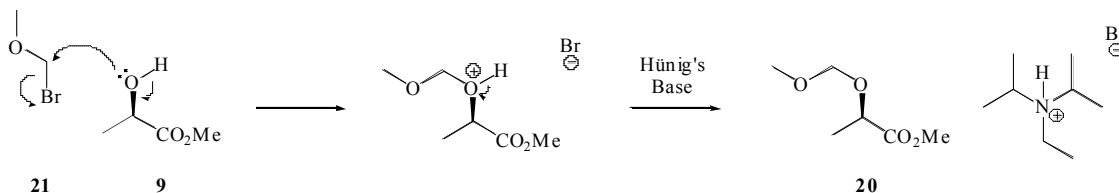


**Figure 16.** S<sub>N</sub>2 pathway for the MOM-protection of (*R*)-methyl lactate

The reaction occurs *via* an associative transition state (Figure 17).

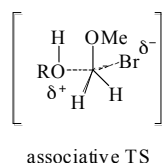


**Figure 17.** S<sub>N</sub>2 reactions proceed *via* an associative transition state.

The rate of this reaction can be expressed as follows: Rate =  $k_{S_{N2}}$  [ROH] [MOMBr]

The second mechanistic possibility for the transformation is also an S<sub>N</sub>2 process, however the nucleophile in this case is the alkoxide anion **9a** and not the alcohol **9** (Figure 18). Clearly, the alkoxide form is much more nucleophilic and as before, the mechanism proceeds via an associative transition state.

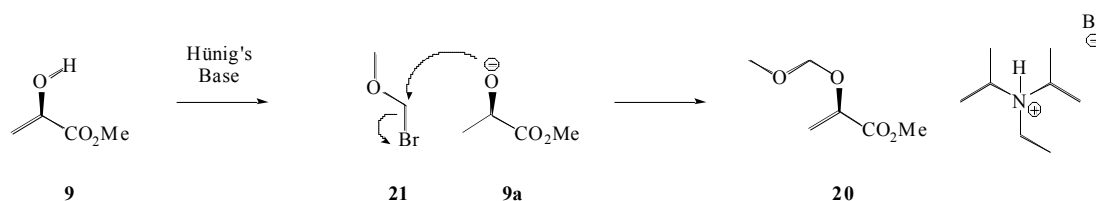


**Figure 18.** S<sub>N</sub>2' pathway for the MOM-protection of (*R*)-methyl lactate

For ease, we shall call this process S<sub>N</sub>2' and we can express the rate of the reaction as: Rate =  $k_{S_{N2}'}$  [ROH] [MOMBr]

The final mechanistic option that can be considered is an S<sub>N</sub>1 process. In this case the rate-determining step is not the nucleophilic attack as with the previous two examples, but the departure of the bromide anion from bromomethyl-methyl ether to form the cationic intermediate **22** (Figures 19 and 20).

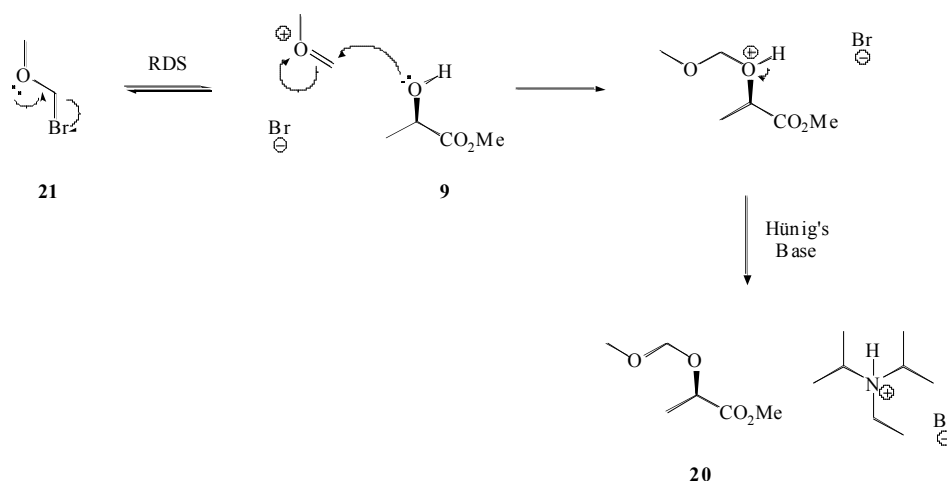


**Figure 19.**  $S_N1$  pathway for the MOM-protection of (*R*)-methyl lactate

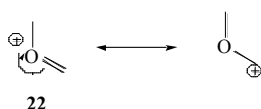


**Figure 20.** The oxonium (**22**) and carbocation resonance forms of the cationic intermediate formed in  $S_N1$  reactions.

The rate for this process is completely independent of the nucleophile and can be expressed as:  $\text{Rate} = k_{S_{N1}} [\text{MOMBr}]$

If one assumes all these processes can take place simultaneously, the overall rate of reaction can be described as:

$$\text{Rate} = k_{S_{N2}} [\text{ROH}] [\text{MOMBr}] + k_{S_{N2}'} [\text{ROH}] [\text{MOMBr}] + k_{S_{N1}} [\text{MOMBr}]$$

However, the reaction is subject to specific conditions which can favour or disfavour the individual processes.

To start with, the presence of the oxygen heteroatom  $\alpha$  to the substitution centre will greatly enhance the  $S_N1$  mechanism. This is due to the stabilisation of the methoxymethyl cation positive charge offered by the oxygen lone electron pairs (Figure 20). Nevertheless, this same effect will also favour an  $S_N2$  reaction proceeding *via* a loose transition state. This pathway is plausible if we employ a good nucleophile such as the alkoxide anion that will react rapidly before bromomethyl-methyl ether dissociates into the methoxymethyl cation and the bromide anion. Therefore, this electronic effect favours  $S_N1$  and  $S_N2'$  but not  $S_N2$ , for which the less nucleophilic alcohol is very unlikely to attack bromomethyl-methyl ether before it dissociates.

However, this situation is reversed under the reaction conditions employed. Firstly, the reaction is carried out in dichloromethane (DCM), a nonpolar solvent. This environment clearly disfavors the  $S_N1$  pathway, which involves the formation of a cation and an anion *via* a transition state that is more polar than the starting materials.

The solvent effect will not relatively have much of an effect on the S<sub>N</sub>2 route and will enhance the S<sub>N</sub>2' process, for which the alkoxide anion is destabilised (i.e. made more reactive) than the transition state (charge delocalisation), reducing the activation energy of the reaction.

Thus, we discard the S<sub>N</sub>1 pathway and are left with the following rate expression:

$$\text{Rate} = k_{S_{N2}} [\text{ROH}] [\text{MOMBr}] + k_{S_{N2}'} [\text{ROH}] [\text{MOMBr}]$$

Although the S<sub>N</sub>2' process seems to be clearly favoured by the above factors, the choice of base disfavours this mechanism. The alcohol and alkoxide anion exist in equilibrium under basic conditions:



Depending on the strength of the base employed, the concentrations of alcohol and alkoxide anion will vary, and therefore also the individual rates of reaction which are dependant upon nucleophile concentration.

The base utilised is Hünig's base or diisopropylethylamine, which has a pK<sub>a</sub> ~11, whereas the secondary alcohol has a pK<sub>a</sub> ~17. Thus, the alcohol form will be predominant and will exist in a 10<sup>6</sup>:1 ratio over the alkoxide form. In the presence of stronger bases such as sodium hydride the equilibrium is shifted towards the alkoxide form.

As a result, the low concentration of alkoxide anion allows us to neglect the S<sub>N</sub>2' pathway, and the rate of reaction can be re-expressed as follows:

$$\text{Rate} = k_{S_{N2}} [\text{ROH}] [\text{MOMBr}] \text{ i.e. the rate of the } S_{N2} \text{ process.}$$

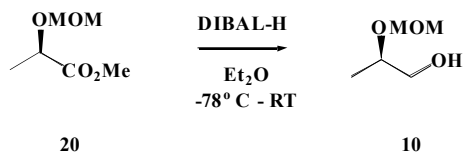
This indicates that the S<sub>N</sub>2 process is almost certainly the predominant route for the methoxymethyl-methyl ether protection of the secondary alcohol in DCM. Nevertheless, one must take into account that the different rate constants could be largely different, which would again change the predominant pathway of reaction. However, these can only be determined experimentally by mechanistic studies.

Concerning the base employed, we can assume that its main role is the removal of hydrobromic acid to form the corresponding ammonium salt (Figures 16/18/19). The reaction proceeded in 45% yield.

The next transformation in the synthetic pathway was the reduction of the ester functionality in **20** to the primary alcohol **10** (Scheme 6). The reducing agent employed was diisobutylaluminium hydride (DIBAL-H), which is known for its ability to reduce esters to alcohols. Also, the fact that the subsequent synthetic step to this reaction is the Swern oxidation of the primary alcohol may make the chosen strategy look unreasonable at first glance. However, previous studies on this section of the synthetic pathway have shown that aldehydes formed at this stage suffer from high volatility and

degradation problems, which are usually accompanied with low yields when the compound is isolated.<sup>25</sup>

Thus, as will be seen later, the chosen synthetic strategy forms and reacts the aldehyde **23** *in situ*, thus avoiding its isolation.



**Scheme 6**

DIBAL-H exists as a bridged dimer and becomes a reducing agent only after forming the Lewis acid-base complex (Figure 21). This aluminium species can reduce the ester group in **20** to the aldehyde **23** at  $-78^{\circ}\text{C}$ . To be precise, the tetrahedral intermediate formed is stable at  $-70^{\circ}\text{C}$  and excess DIBAL-H can be quenched with acid so that the tetrahedral intermediate collapses to the aldehyde on warming to room temperature and with no more reducing agent present. In the reduction carried out, the tetrahedral intermediate was allowed to collapse to the aldehyde **23** with no quenching of the reducing agent. The aldehyde then coordinates a second equivalent of DIBAL-H and the hydrogen atom is delivered to yield a new tetrahedral complex. The tetrahedral aluminium complex was broken down upon treatment with ammonium chloride and the primary alcohol **10** was obtained in 68% yield. The reaction was carried out in diethyl ether ( $\text{Et}_2\text{O}$ ).

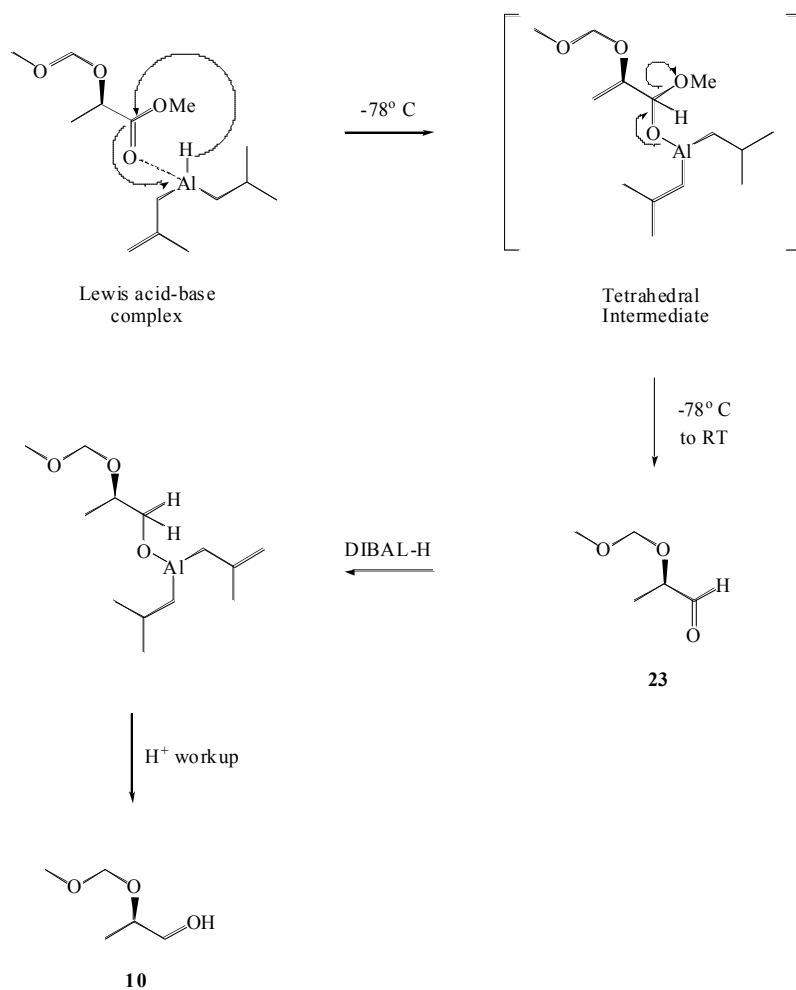
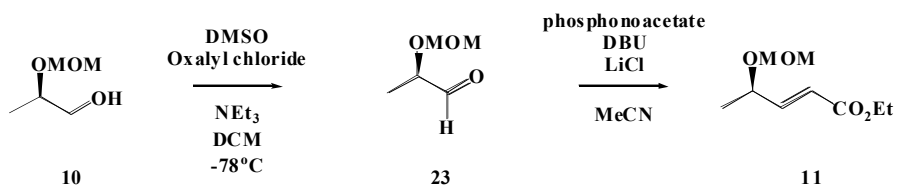


**Figure 21.** DIBAL-H reduction of an ester to an alcohol.

The following conversion in the synthetic route involves a one-pot Swern oxidation / Horner-Wadsworth-Emmons reaction of the primary alcohol **10** to the allylic ester **11** via the *in situ* generation of the aldehyde **23** (Scheme 7).



**Scheme 7**

The first part of this double reaction, i.e. the Swern oxidation, proceeds by the mechanism shown below (Figure 22).

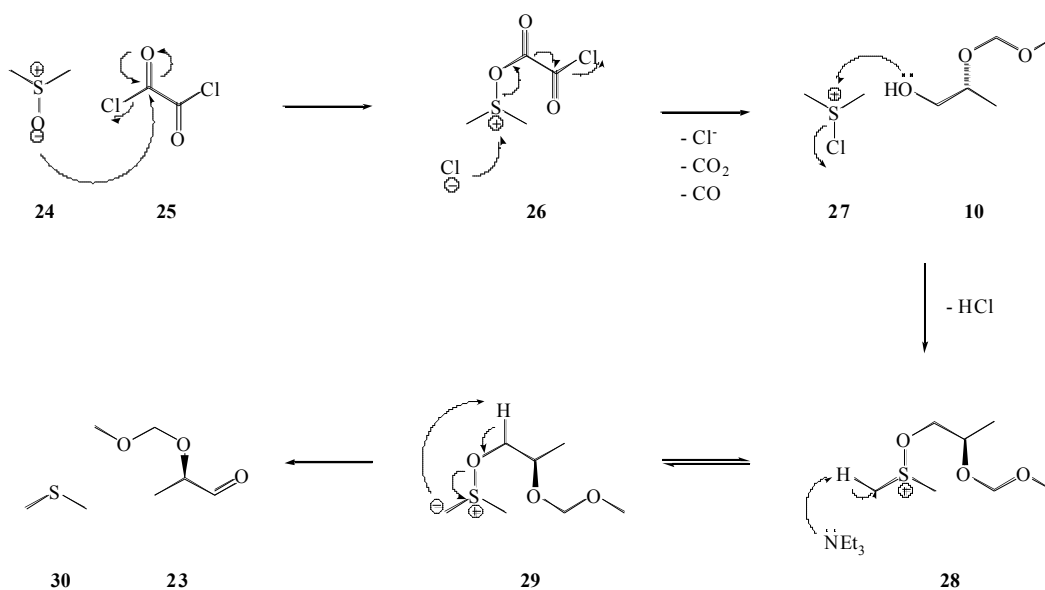


**Figure 22.** Mechanism of Swern oxidation.

The initial step of the Swern oxidation mechanism is the nucleophilic attack of dimethyl sulfoxide (DMSO) **24** on oxalyl chloride **25** to yield the electrophilic sulfonium species **26** and a chloride anion. It is the chloride anion itself which attacks the sulfonium centre to expel a remarkable leaving group that fragments into three different species: carbon dioxide ( $\text{CO}_2$ ), carbon monoxide ( $\text{CO}$ ) and a chloride anion. Clearly, it is entropy that drives this fragmentation irreversibly to completion, not only because two molecules generate four molecules, but also because two out of these four newly generated molecules are in the gaseous state ( $\text{CO}_2$  and  $\text{CO}$ ).

It is at this stage that the primary alcohol **10** comes into play. The chlorosulfonium ion **27** is attacked by the alcohol to form yet another sulfonium species **28**, which is stable enough to be deprotonated by base. Deprotonation of the sulfonium  $\alpha$ -centre with triethylamine yields the diionic species **29**. A concerted process then takes place to generate the aldehyde **23** and dimethyl sulphide **30**.

Overall, this process is a redox reaction in which the alcohol is oxidised to the aldehyde and DMSO is reduced to dimethyl sulphide.

Bearing in mind that the stereochemistry of the chiral ether is crucial towards the synthesis of a specific diastereomer of the conhydrine analogue, it may strike as dangerous to form an aldehyde with a stereocentre at the  $\alpha$ -position of a carbonyl, especially after a stage that involves an excess of base. However, the  $\text{pK}_a$  of triethylamine is  $\sim 11$  and that of a carbonyl  $\alpha$ -hydrogen is  $\sim 20$ , which means that about 1 in  $10^9$  aldehyde molecules will be deprotonated. Therefore, racemisation at the chiral centre can be neglected.

In a separate vessel, and while the aldehyde is being formed, triethyl phosphonoacetate **31** is deprotonated by 1,8-diazabicyclo[5.4.0]undecene-7 (DBU) in acetonitrile (MeCN) to give the nucleophilic enolate species **32** (Figure 23).

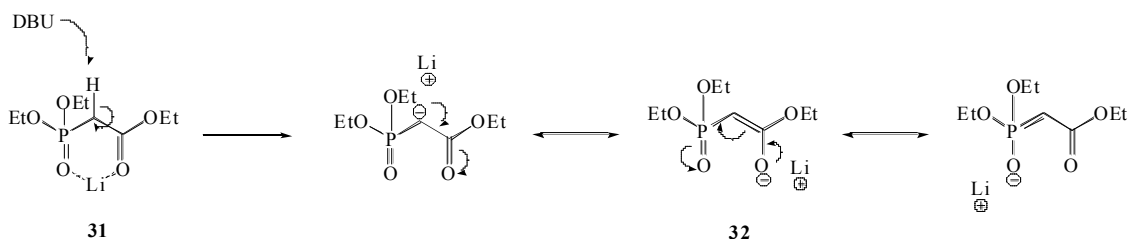


**Figure 23.** Formation of the nucleophilic species for the Horner-Wadsworth-Emmons reaction. See later for DBU structure.

The formation of the lithium enolate species is enhanced by employing lithium chloride. The lithium cation coordinates to the oxygen atoms of the carbonyl and phosphoryl centres and acts as a Lewis acid by pulling electronic density and making the shared carbonyl and phosphoryl  $\alpha$ -centre more electron deficient. The result is more acidic  $\alpha$ -hydrogens, which enables the use of weak or uncharged bases such as DBU (uncharged).

The nucleophilic lithium enolate species is then reacted with the aldehyde product in the Swern oxidation reaction mixture to give the *E*-allylic ester **11** as the major reaction product. The mechanism for this stage of the reaction is shown below (Figure 24).

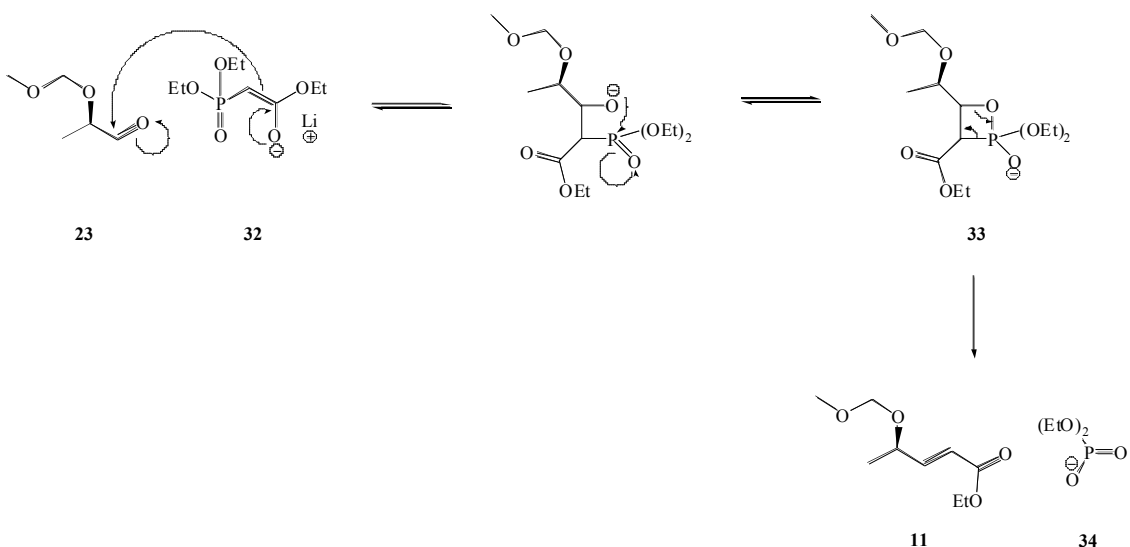


**Figure 24.** Mechanism for the second stage of the Horner-Wadsworth-Emmons reaction.

The resonance forms of the nucleophilic enolate enable a slower but reversible reaction pathway that proceeds *via* a late planar transition state and leads to the thermodynamic *E*-allylic ester. The contrasting picture would involve a nucleophile in which the charge is completely localised, making the nucleophile very reactive and leading to a rapid reaction proceeding *via* an early puckered transition state yielding the kinetic *Z*-isomer (Figure 25).

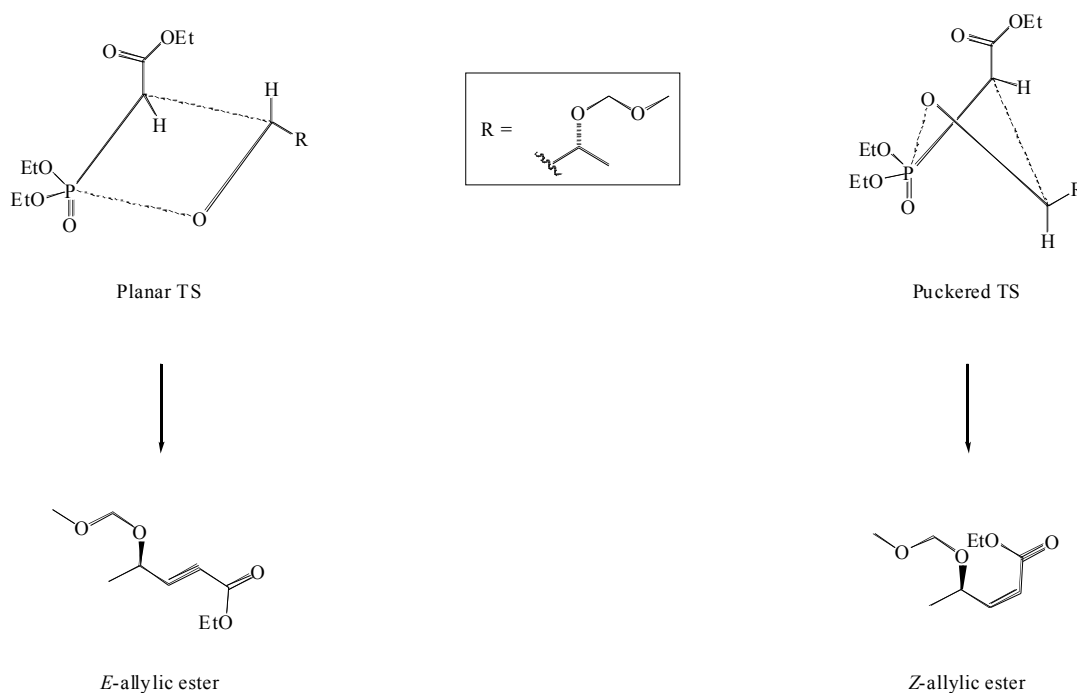
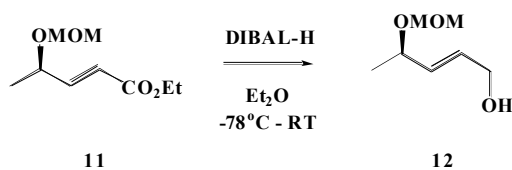


**Figure 25.** Thermodynamic (left) and kinetic (right) pathways for the formation of *E* and *Z* alkenes in the Horner-Wadsworth-Emmons reaction. In both cases the least sterically-impeded pathway is shown.

The steps that follow the nucleophilic attack are formation of the oxaphosphetane complex **33**, and its breakdown to yield the *E*-allylic ester **11** predominantly and the water-soluble by-product **34**. The irreversibility of this step is due to the strong covalent double bond formed between phosphorus and oxygen, which drives the reaction to completion.

The transformation from the primary alcohol **10** to the *E*-allylic ester **11** proceeded in an overall 63% yield. It is worth underlining that the Horner-Wadsworth-Emmons reaction is stereoselective and not stereospecific, and therefore a small amount of the *Z*-alkene is formed. In this case, a 53:1 ratio of *E*:*Z* isomers was obtained, the amount of *Z*-alkene being so low it was neglected, and isolation of the *Z*-isomer was not attempted (Appendix).

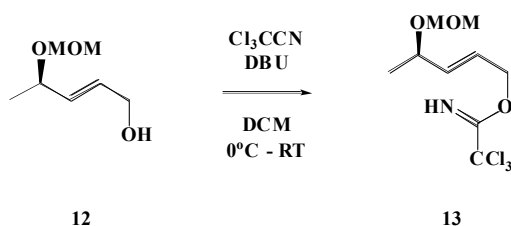
The next transformation is the reduction of the ester functionality in **11** to the allylic alcohol **12**, once again employing DIBAL-H as the reducing agent (Scheme 8).



**Scheme 8**

The mechanism of this reaction is identical to that of the previous reduction and will not be discussed again. However, in this case the reduction to the alcohol is not a strategy to avoid the isolation of the aldehyde as was the case previously. The conversion took place in 75% yield with no trace of the aldehyde intermediate found.

The following conversion involved the preparation of the trichloroacetimidate substrate **13** for the crucial palladium-catalysed aza-Claisen rearrangement (Scheme 9). Until this stage, the isolation of intermediates in the synthetic pathway suffered from the volatility of the product, which is usually reflected on the lower than expected yields. However, from the formation of the trichloroacetimidate onwards this is no longer a problem, as all intermediates are non-volatile.



**Scheme 9**

As in the Horner-Wadsworth-Emmons reaction, the base employed for this reaction is the amidine DBU. With a pKa of  $\sim 12.4$ , amidines are stronger bases than amines, however amidine bases are uncharged. In an amidine one nitrogen atom is  $sp^2$  hybridised and the other is  $sp^3$  hybridised. One would expect the  $sp^3$  centre to be more basic but it is in fact at the  $sp^2$  that protonation occurs. However, both nitrogen electron lone pairs are involved in the protonation process. Thus, the positive charge formed on protonating can be delocalised onto both nitrogen centres (Figure 26).

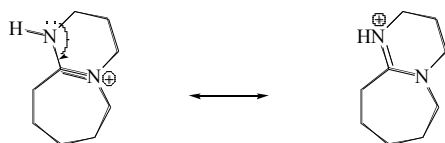


**Figure 26.** The positive charge created upon protonation can be delocalised onto both nitrogen centres in amidines (DBU shown).

Stoichiometric amounts of DBU were used for the reaction but it is worth mentioning that the same transformation was very recently carried out by the Overman group under catalytic amounts of the same base.<sup>26</sup> The mechanism of the reaction is shown below (Figure 27). Although the main reaction pathway probably involves nucleophilic attack from the alcohol group and then deprotonation (the pKa of an allylic alcohol is  $\sim 15.5$  and that of DBU is  $\sim 12.4$ ), the inverse sequence is shown. This makes it easier to appreciate the catalytic nature of DBU in the reaction.

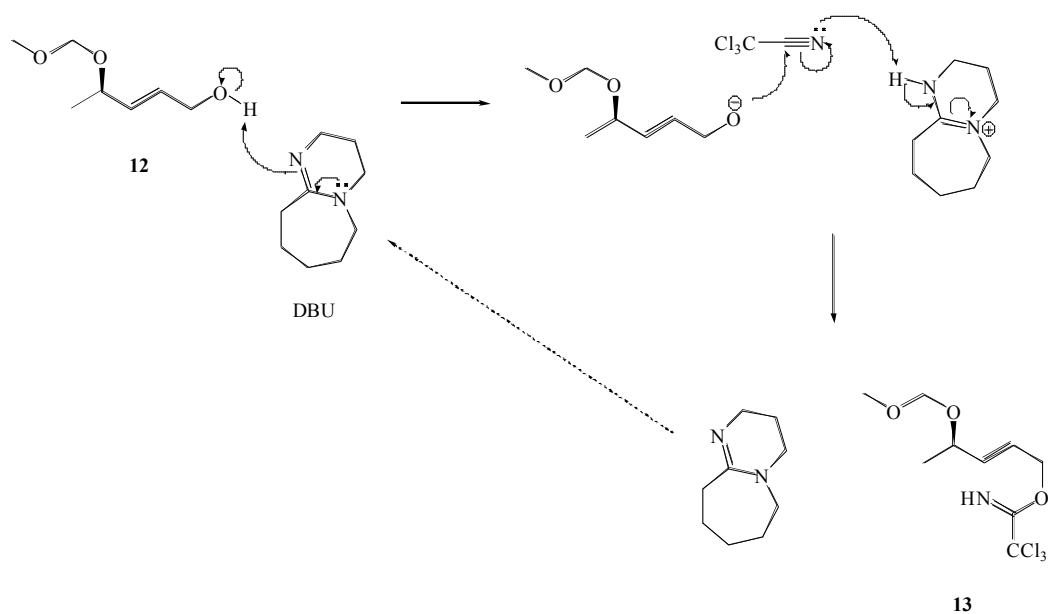
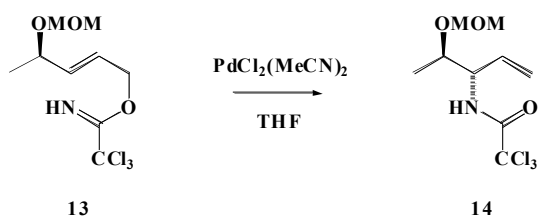


**Figure 27.** Mechanism for the formation of trichloroacetimidates from allylic alcohols in the presence of catalytic DBU.

Once the allylic alcohol **12** has attacked a trichloroacetonitrile molecule, the protonated DBU molecule delivers its proton to the nitrile group, resulting in the formation of the trichloroacetimidate **13** and a regenerated neutral molecule of DBU. The allylic trichloroacetimidate compound formed is believed to be unstable, therefore workup was simple and rapid (see experimental section), and the rearrangement to the trichloroamide was set up immediately after isolation of the trichloroacetimidate.

The ether-directed, palladium-catalysed aza-Claisen rearrangement of trichloroacetimidates into trichloroamides (e.g Scheme 10) was covered in detail in the introduction essay to the project, however the importance of this step within the total synthesis of the conhydrine analogue requires the main points of the rearrangement to be recapitulated.



**Scheme 10**

The initial interest in the process arose from the need of accessing allylic amines from more readily available allylic alcohols.<sup>27</sup> Overman reported the clean [3,3]-sigmatropic rearrangement of different trichloroacetimidates into trichloroamides under thermal conditions, e.g. **35** into **36** (Figure 28).

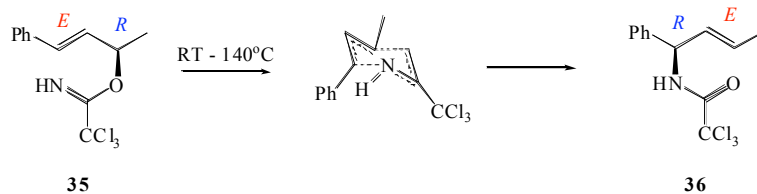


**Figure 28.** Thermal rearrangement of trichloroacetimidates into trichloroamides.

The need for milder reaction conditions resulted in the investigation of metal catalyses applied to the rearrangement.<sup>28</sup> Palladium and mercury salts were shown to work best, and interestingly, the behaviour of palladium(II) and palladium(0) complexes was resulting in different outcomes. Palladium(II) complexes give solely [3,3] Claisen product whereas palladium(0) catalysts result in mixtures of [3,3] Claisen and [1,3] anti-Claisen products (Figure 29).

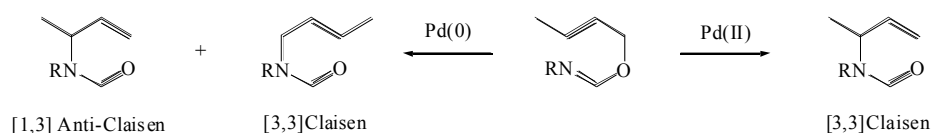


**Figure 29.** The rearrangement of trichloroacetimidates into trichloroamides in the presence of palladium(II) or palladium(0) results in different reaction outcomes.

It is necessary to understand the mechanism underlying these two processes, which cannot simply be defined as [3,3] sigmatropic rearrangements due to the involvement of a palladium complex which makes the processes non-concerted.

In the case of the palladium(II)-catalysed process, a cyclisation induced rearrangement occurs (Figure 30).

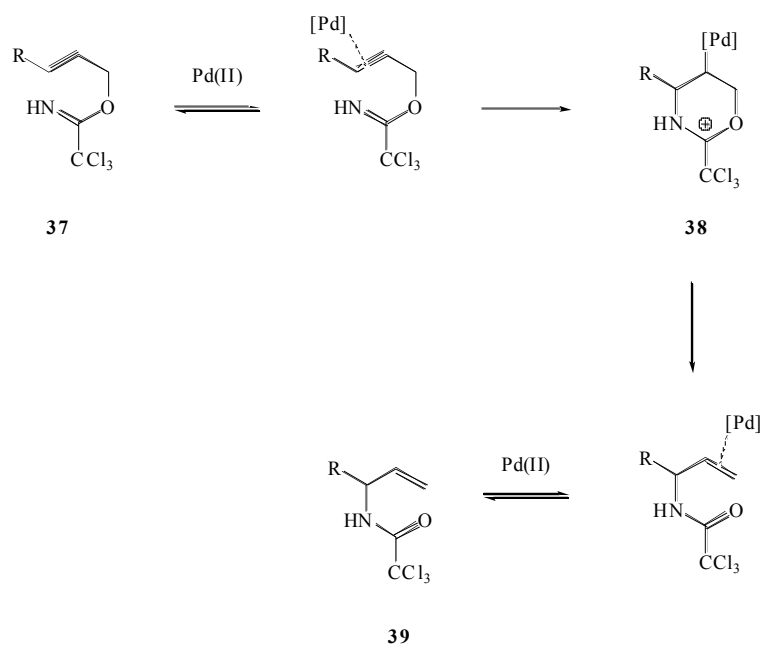


**Figure 30.** Palladium(II)-catalysed rearrangement of trichloroacetimidates into trichloroamides.

The palladium complex coordinates the alkene in **37** with a subsequent aminopalladation of the alkene to give the cationic cyclic intermediate **38**. This intermediate then rapidly undergoes reductive elimination and dissociation from the metal complex to yield the amide product **39** and regenerate the catalyst.

On the other hand, the rearrangement of trichloroacetimidates under palladium(0) catalysis is believed to proceed *via* a  $\pi$ -allyl complex that generates the trichloroacetimidate anion as a leaving group (Figure 31).

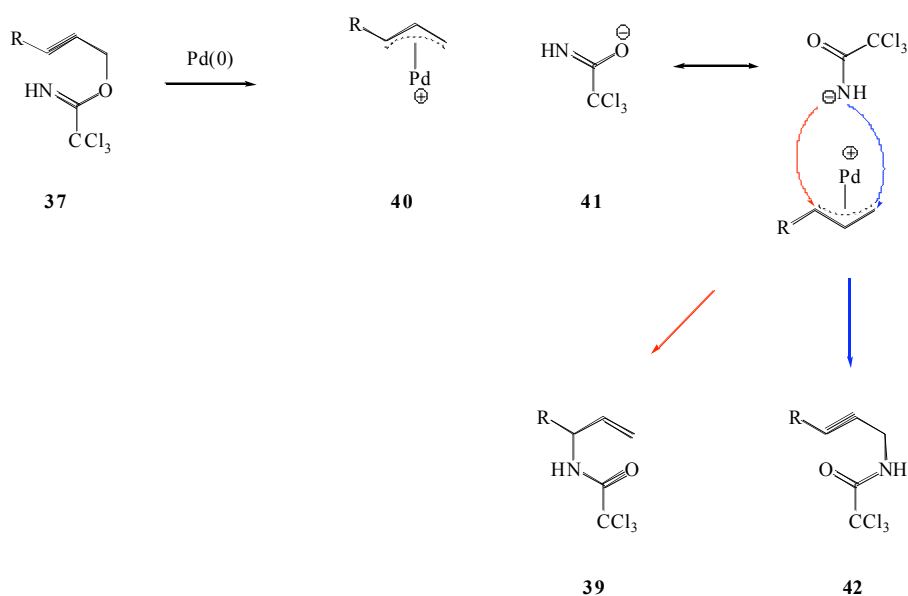


**Figure 31.** Palladium(0)-catalysed rearrangement of trichloroacetimidates into trichloroamides.



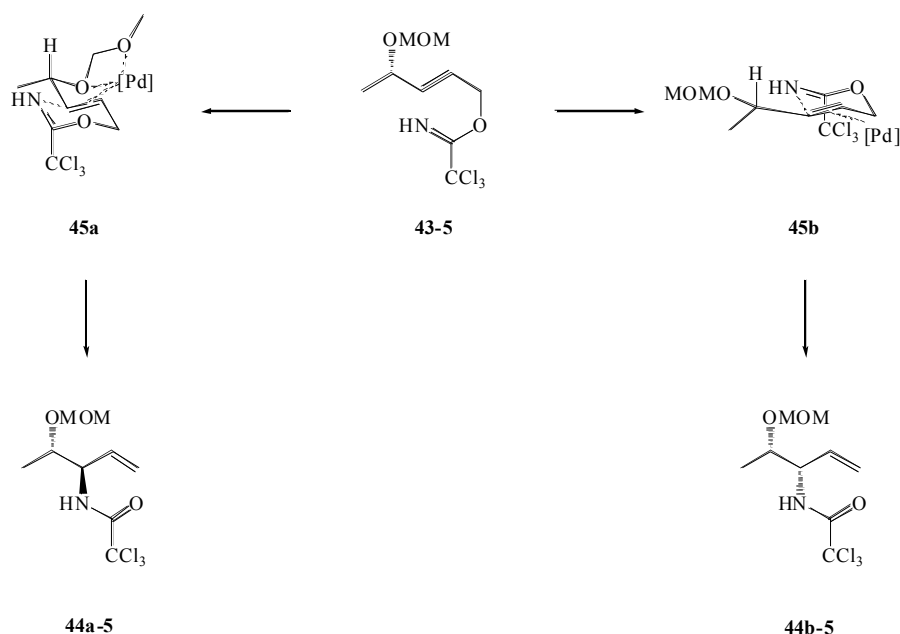
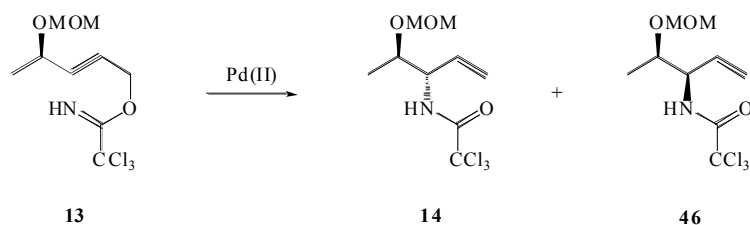


**Figure 32.** The differential facial coordination of palladium leads to different diastereomers.

The stereoselective process is based on the coordination of the palladium(II) species to a chiral group within the trichloroacetimidate **43-5**, which coordinates to the metal catalyst from one face of the molecule only. This face then becomes sterically and electronically crowded, and likewise the also palladium-coordinated alkene is attacked by the acetimidate nitrogen unilaterally. This is easily explained by illustration of the chair conformation transition states in the rearrangement. Intermediate **45a** shows the palladium atom coordinated from the backside of the molecule, as directed by the ether group. This forces nucleophilic attack to occur from the front face, leading to the *anti* diastereomer **44a-5**. However, it is possible that the palladium atom does not coordinate to the ether group but instead coordinates the alkene from the less hindered front face, giving the intermediate **45b**. In this case, nucleophilic attack will come from the back face and will result in the formation of the *syn* diastereomer **44b-5**.

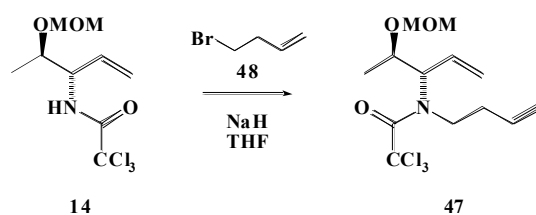
The rearrangement carried out in this project yielded the *anti* diastereomer in 43% yield and 82% diastereomeric excess (Scheme 11 and Appendix).



**Scheme 11.** The ether-directed, palladium(II)-catalysed rearrangement in the project resulted in a 10:1 *anti:syn* (**14:46**) product mixture.

Once the rearrangement was successfully performed and the stereochemistry in the target molecule of the synthetic pathway was set up, it became a matter of introducing the second terminal alkene group to form the substrate of the ring-closing metathesis step.

In an attempt to make the synthetic route one step shorter, and predicting the trichloroamide group would not affect ring-closing metathesis, the direct alkylation of the trichloroamide **14** to the di-alkene species **47** was tested (Scheme 12). Even though one would expect the electron-withdrawing effect of the trichloroamide group to hinder the reaction by reducing the nucleophilicity of the nitrogen atom, literature precedence indicated the reaction was feasible.<sup>30,31</sup>

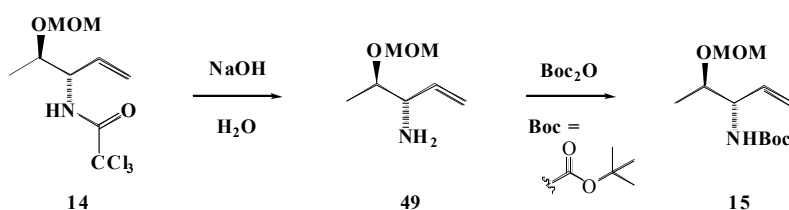


Scheme 12

Sodium hydride, a strong base, was chosen in order to deprotonate the trichloroamide and to form the nucleophilic anion. However, the trichloroamide did not react with 4-bromobutene **48**, presumably, at least in part, due to the electron deficient nature of the trichloroamide.

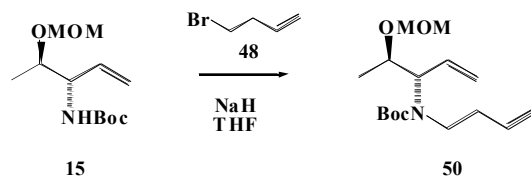
Related literature precedent for the failure of the direct homoallylation of trichloroamides is known, and in many cases alkylation is achieved *via* the protection of the free amino compound **49** as a carbamate, which was the initial idea behind the proposed synthetic pathway.<sup>32</sup>

Following the initial strategy, the trichloroamide group in **14** was rapidly cleaved in sodium hydroxide and water to yield the free amine **49** which was then treated in the same solution with butyloxycarbonyl (Boc) anhydride to yield the butyloxycarbonyl carbamate **15** (Scheme 13). The mechanism for the process is a simple hydrolysis of the amide bond, enabled by the electron-withdrawing character of the trichloromethyl group, followed by a standard substitution reaction at the anhydride carbonyl centre. The two-step conversion was carried out in an overall 55% yield.



Scheme 13

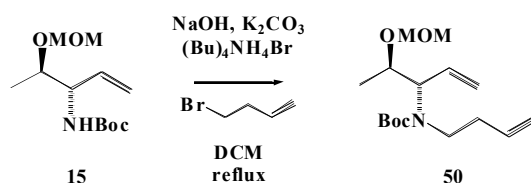
The first method employed in the homoallylation of the Boc-carbamate **15** was the same method that was used for the alkylation attempt of the trichloroamide (Scheme 14). However, as had previously occurred, no reaction took place and the starting material was recovered.



Scheme 14

Different strategies followed in an attempt to obtain the homoallylated product.

Firstly, possible solubility problems were tackled by employing the phase transfer catalyst tetrabutylammonium bromide (Scheme 15). Following literature protocol, sodium hydride and potassium carbonate were utilised to form the anion, which would then react with 4-bromobutene to give the di-alkene species **50**.<sup>33</sup> Unfortunately, only starting material was recovered.



Scheme 15

The next attempt at alkylating the Boc-carbamate focused on the electrophile rather than the nucleophile. The homoallyl group does not possess the electronic resonance of an allyl group (Figure 33).

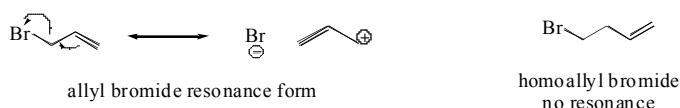
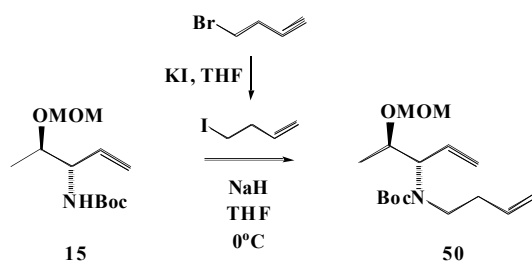


Figure 33. A contrast between the allyl and homoallyl groups.

In the case of the allyl bromide species, the departure of bromide is enhanced by the delocalisation of the positive charge generated, thus maximising the chances of an S<sub>N</sub>1 or S<sub>N</sub>2 (*via* loose transition state) reaction. The homoallyl group cannot induce these processes due to the lack of resonance forms. With this in mind, it was necessary to activate the electrophile by other means.

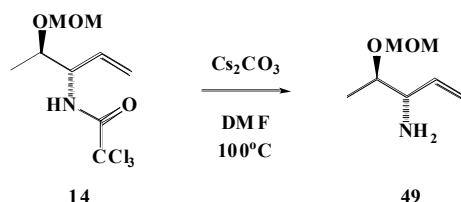
The method of choice was iodide nucleophilic catalysis (Scheme 16). The requirements for this method to work are a substrate with a better leaving group than iodide and an incoming nucleophile more nucleophilic than iodide. In this case, 4-bromobutene can lose bromide in the presence of iodide to give 4-iodobutene, which can lose iodide in the presence of the Boc-carbamate anion. However, no reaction was observed.



Scheme 16

The failure to alkylate the *N*-BOC compound **15** despite the different methods carried out meant that other strategies were required. The initial synthetic route was once again altered and it was decided that alkylation would be tried directly on the free amino compound **49**.

A second batch of trichloroamide was deprotected, this time employing a recently published method based on caesium carbonate, which, compared to potassium carbonate, includes a much softer and therefore less basic cation (Scheme 17).<sup>34</sup>



Scheme 17

The mechanism of this process proceeds *via* the anhydride **51**, which is hydrolysed upon workup (Figure 34).

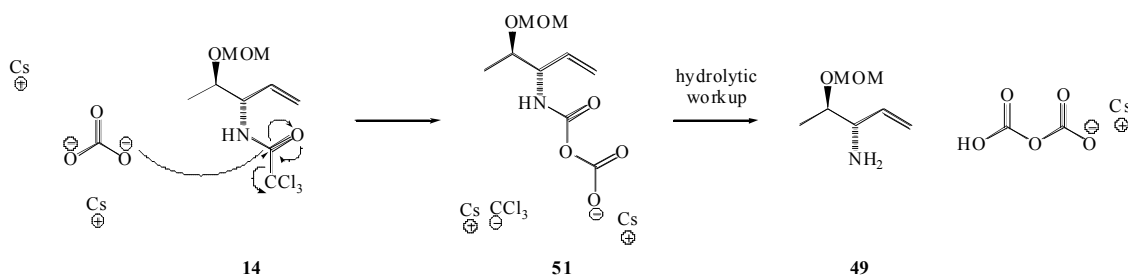
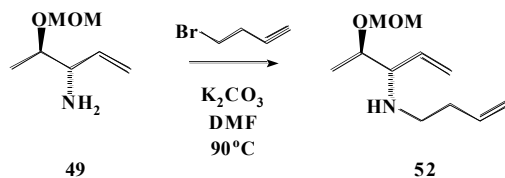


Figure 34. Mechanism for the caesium carbonate deprotection of trichloroamides.

The formation of the amine was monitored very clearly by thin layer chromatography (free amino compound is barely shifted from the baseline), and once the conversion was complete, 4-bromobutene and potassium carbonate were added to the reaction mixture (Scheme 18).



**Scheme 18**

Although the inductive effect of alkyl groups would lead to think that the process would not stop at the monoalkylation stage, as the monoalkylated product is easier to alkylate than the free amine, and then the dialkylated product is much easier to quaternise than to alkylate the free amine, related literature precedence indicated monoalkylation was feasible under standard alkylation conditions (Figure 35).<sup>35</sup>

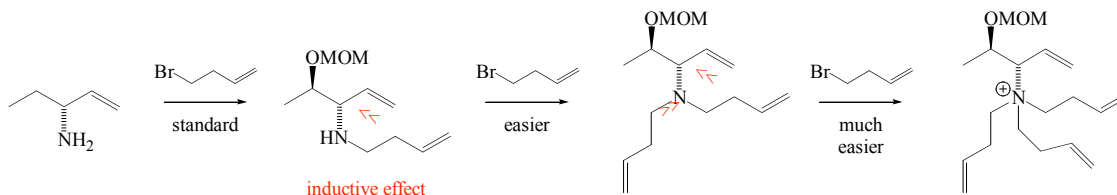
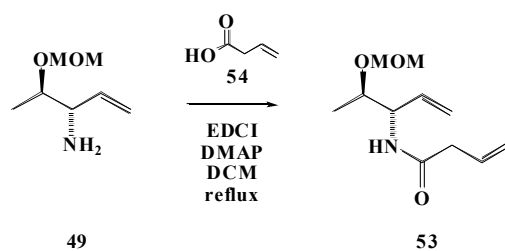


**Figure 35.** Mono-, di- and tri-alkylation of a primary amine.

In any case, none of these occurred and the crude amine compound was recovered and subjected to similar alkylation conditions, this time with triethylamine as base. Again, no reaction was observed.

In sight of the results obtained, alkylation was no longer pursued. Instead, acylation was the strategy chosen. The implications of acylating instead of alkylating meant a further step in the synthesis of the conhydrine analogue would be required, in particular a reduction of the amide/lactam functionality to the amine/piperidine. In the case acylation were successful, literature precedent indicated that the resulting amide functionality would not affect ring-closing metathesis.<sup>36</sup> From a pharmacological point of view, the possibility of introducing a lactam as an analogue of a piperidine can even be seen as a benefit, e.g. to prevent *N*-dealkylation metabolic processes.

The first acylation method that was carried out was an *N*-(3-dimethylaminopropyl)-*N*-ethylcarbodiimide (EDCI) coupling of the amine **49** and vinylacetic acid **54** employing 4-dimethylaminopyridine (DMAP) as a nucleophilic catalyst (Scheme 20).<sup>37</sup>



**Scheme 20**

There are three stages to the coupling mechanism (Figure 36). First of all, DMAP attacks the carbodiimide centre of EDC to yield the guanidine intermediate **55**, which becomes a much more activated electrophile than EDC itself. Vinylacetic acid then attacks the guanidine carbon centre to generate the new complex **56** with displacement of DMAP, which is regenerated. The amine then comes into play and attacks the carbonyl centre of intermediate **56** to displace the urea leaving group **57** and the acylated reaction product **53**.

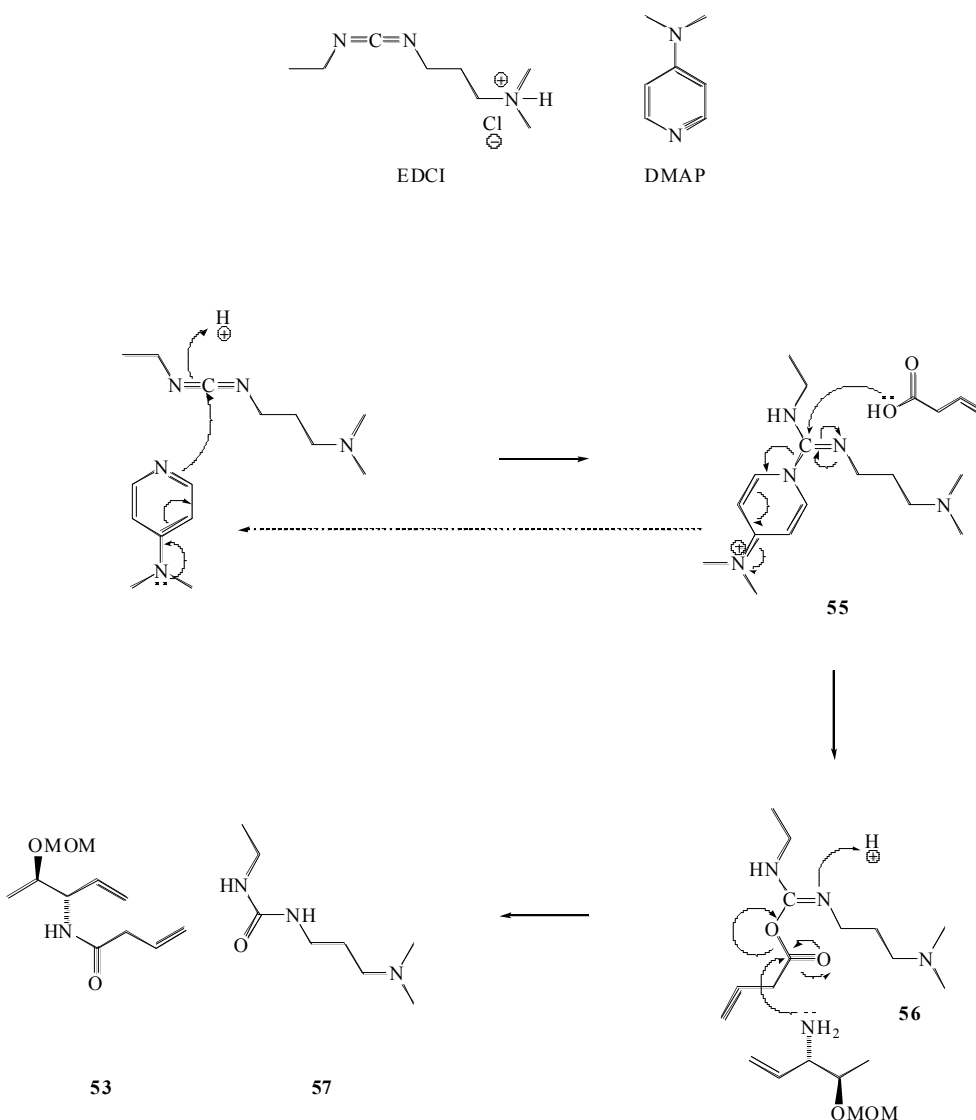
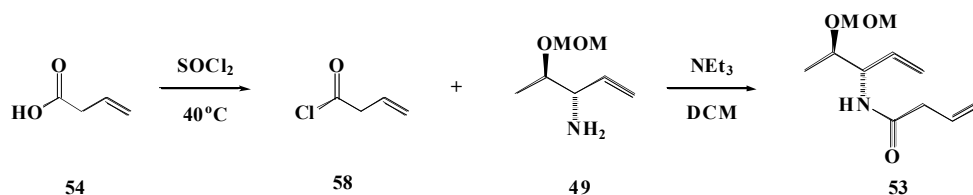


**Figure 36.** Structures of EDCI (provided as HCl salt from commercial sources) and DMAP (top) and mechanism of an amine-acid EDCI, DMAP-catalysed coupling.

Unfortunately, only starting material was recovered from the reaction mixture despite prolonged periods of refluxing. One of the reasons for the failure of this method could be the large steric bulk created by EDC and the intermediate it forms with the acid, which can potentially impede access of the amine to the carbonyl centre in the crucial step of the reaction.

Based on the results obtained up to this stage, a possible explanation for the lack of reactivity of the allylic amine could be a steric impediment imposed on the nucleophilic nitrogen atom by the allyl and MOM groups. This steric hinderance would lead to a much-reduced nucleophilic character of the amine group, however there are many literature examples where similar, or even more sterically congested related compounds were alkylated without a problem. Taking this hypothesis of steric grounds into account, acylation with a smaller substrate than the EDC complex should have more chances of proceeding.



**Scheme 21**

As a final attempt, the acylation of the allylic amine **49** with the corresponding acyl chloride **58** of vinylacetic acid **54** was pursued (Scheme 21). Vinylacetic acid was converted to 3-butenoyl chloride in the presence of thionyl chloride in 51% yield employing fractional distillation as the method of purification. The allylic amine was then reacted with 3-butenoyl chloride employing triethylamine as base for the reaction.

In this case, the outcome of the reaction was interesting. Indeed, acylation was achieved with the formation of amide rotomers, however the methoxymethyl protecting group had been removed. The nature of the side reaction can be explained by the order in which reagents were added: the acyl chloride with the amine with 30 minutes of stirring followed by the addition of triethylamine. As can be seen below, the reaction of the first two species in the absence of base generates hydrochloric acid, which has the potential of deprotecting the secondary alcohol group (Figure 37).

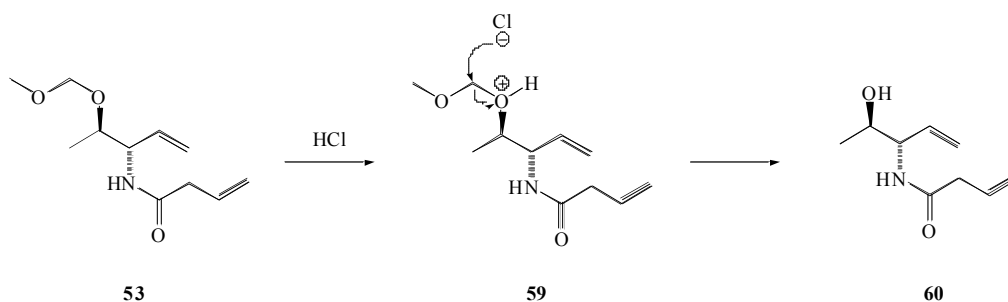


**Figure 37.** Mechanism of MOM-deprotection.

It is believed the species isolated was not **53**, but the MOM-deprotected analogue of it **60** below (Figure 38). This compound was isolated in a moderate 30% yield.

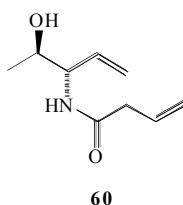


**Figure 38**

## Future Work

It would certainly be interesting to repeat the reaction in the initial presence of excess triethylamine. In any case, if the secondary alcohol were still obtained, there is no reason to believe the hydroxyl would interfere with the final steps of the synthetic pathway. It is known that ring-closing metathesis tolerates this functionality, therefore the formation of the six-membered piperidine core should proceed by the catalytic cycle shown below (Figure 39).<sup>38</sup>

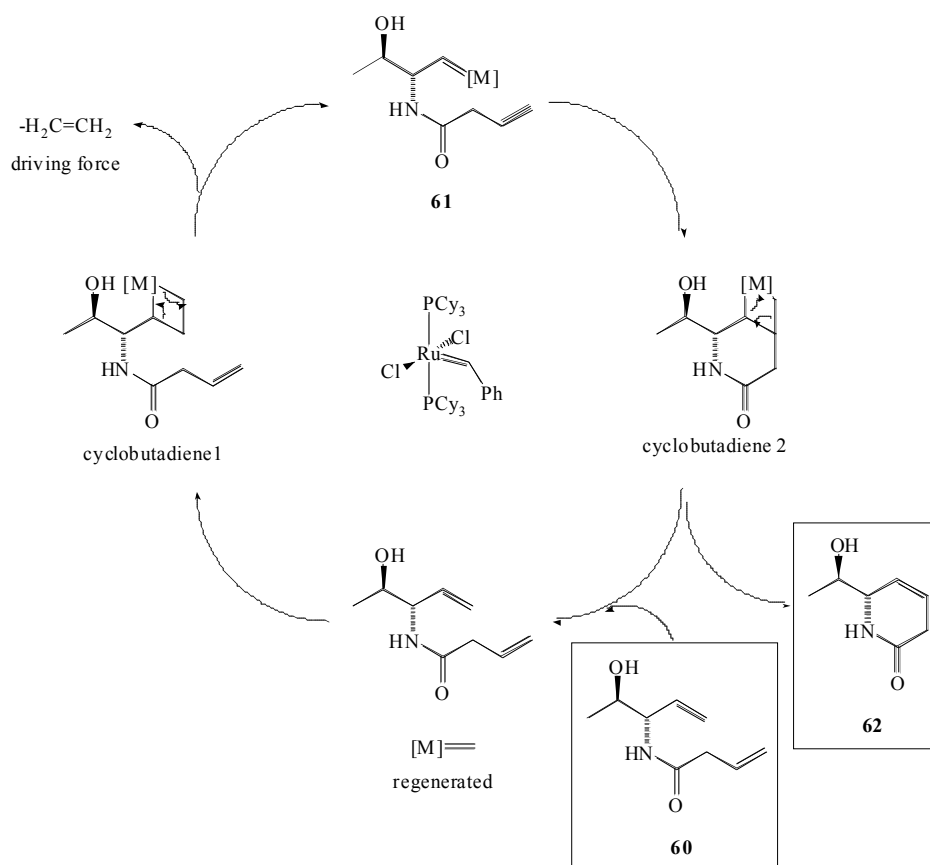
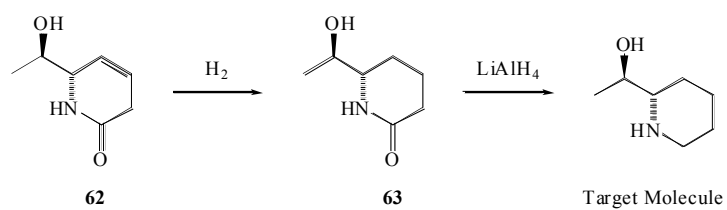


**Figure 39.** Predicted RCM catalytic cycle of the isolated di-alkene species **60**. The second generation Grubbs catalyst is illustrated in the centre of the catalytic cycle.

The catalytic cycle represents the propagation step of the RCM process (the initiation step occurs with loss of styrene instead of ethylene). Di-alkene species **60** undergoes metathesis with methylidene to generate the first metallacyclobutane, which forms a new alkylidene complex **61** via a [2+2] cycloaddition. This process is driven to completion by the loss of volatile ethylene. Complex **61** then undergoes an intramolecular RCM via a second metallacyclobutane intermediate to yield the unsaturated lactam product **62** and to regenerate the catalytic methylidene species.

The final steps of the synthetic pathway involve the reduction of the unsaturated lactam to the piperidine core of the (+)- $\alpha$ -conhydrine analogue. This is achieved by

hydrogenation of the double bond in **62** to yield lactam **63** followed by reduction of the amide functionality in **63** to the corresponding amine, i.e. the analogue of (+)- $\alpha$ -conhydrine (Scheme 22).



**Scheme 22.** Predicted final steps in the synthesis of the target molecule.

## Conclusion

Significant progress towards the synthesis of the analogue of (+)- $\alpha$ -conhydrine was achieved.

The introduction of the crucial second stereocentre was successfully carried out employing the ether-directed, palladium(II)-catalysed aza-Claisen rearrangement.

However, problems were encountered in the homoallylation of the rearrangement product for the introduction of the second alkene group required for ring-closing metathesis. The lack of reactivity of the trichloroacetamide, carbamate, and free amine compounds lead to a change in the synthetic strategy. Acylation, and no longer alkylation, was pursued.

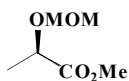
Finally, acylation with 3-butenoyl chloride was achieved, although due to the parallel cleavage of the methoxymethyl ether protecting group, the method is still to be further examined.

Future work will involve the completion of the total synthesis of the analogue of (+)- $\alpha$ -conhydrine as well as the application of the chemistry developed to the total synthesis of (+)- $\alpha$ -conhydrine itself, and possibly other natural products or bioactive compounds such as azasugars.

### 3. Experimental

Reagents were purchased from commercially available sources. (*R*)-(+)-methyl lactate, the initial substrate of the synthetic pathway, was purchased from Sigma Aldrich. Solvents employed were obtained from dry and distilled sources. All reactions were performed under an atmosphere of nitrogen and in an anhydrous vessel environment (flame-drying or oven-drying at 110 °C). Fischer Matrex silica 60. Macherey-Nagel aluminium backed plates pre-coated with silica gel 60 (UV<sub>254</sub>) were employed for thin layer chromatography, which was monitored with a UV Mineralight device or by oxidative staining with a 0.5% potassium permanganate, 2.5% sodium hydrogen carbonate aqueous solution. Fourier transform infrared spectroscopy was performed on a Nicolet Impact 410 or Jasco FT/IR-410 device employing NaCl discs (oils) or pressurised CsI films (solids). Optical rotation measurements (in 10<sup>-1</sup> deg cm<sup>2</sup> g<sup>-1</sup>) were obtained from a POLAAR 200, AA Series Automatic Polarimeter device. <sup>1</sup>H Nuclear Magnetic Resonances were recorded on Bruker<sup>®</sup> DPX 100 Hz and 400 Hz spectrometers with chemical shifts given in parts per million (ppm) and employing deuterated chloroform as a standard reference peak at 7.26 ppm. The same equipment was utilised to carry out <sup>13</sup>C Nuclear Magnetic Resonances. Mass spectrometry was carried out on a Joel M-station JMs 700, Dual Sector, High Resolution, Mass Spectrometer.

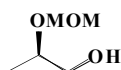
#### Methyl (2*R*)-2-Methoxymethoxypropanoate (**20**)<sup>39</sup>



20

*N,N*-Diisopropylethylamine (7.69 cm<sup>3</sup>, 43.2 mmol) and bromomethyl methyl ether (90%, 3.92 cm<sup>3</sup>, 43.2 mmol) were added to a solution of Methyl-(*R*)-(+)-methyl lactate (2.75 cm<sup>3</sup>, 28.8 mmol) in dichloromethane (45 cm<sup>3</sup>). The reaction mixture was heated under reflux overnight and was then diluted with dichloromethane (20 cm<sup>3</sup>) and washed with 2 M hydrochloric acid solution (20 cm<sup>3</sup>). The organic layer was washed with 2 M hydrochloric acid solution (3 x 20 cm<sup>3</sup>), dried (MgSO<sub>4</sub>), filtered and evaporated *in vacuo*. Purification was carried out by flash column chromatography using an elution gradient of diethyl ether-petroleum ether (0%-35%) to give Methyl (2*R*)-2-methoxymethoxypropanoate (**20**) (1.9 g, 45%) as a colourless oil. [ $\alpha$ ]<sub>D</sub><sup>15</sup> +100.4 (*c* 1.0, CHCl<sub>3</sub>); lit.<sup>39</sup> [ $\alpha$ ]<sub>D</sub><sup>24</sup> +85.5 (*c* 1.0, CHCl<sub>3</sub>);  $\delta$ <sub>H</sub> (400 Hz, CDCl<sub>3</sub>) 1.44 (3H, d, *J* 6.8 Hz, 3-H<sub>3</sub>), 3.39 (3H, s, OCH<sub>2</sub>OCH<sub>3</sub>), 3.75 (3H, s, OMe), 4.25 (1H, q, *J* 6.8 Hz, 2-H), 4.69 (1H, d, *J* 2.0 Hz, OCHHO), 4.704 (1H, d, *J* 2.0 Hz, OCHHO);  $\delta$ <sub>C</sub> (100 MHz, CDCl<sub>3</sub>) 18.5 (CH<sub>3</sub>), 52.02 (CH<sub>3</sub>), 55.86 (CH<sub>3</sub>), 71.45 (CH), 95.87 (CH<sub>2</sub>), 173.5 (CO); *m/z* (CI) 149.16.

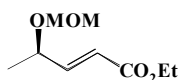
### (2*R*)-2-Methoxymethoxypropan-1-ol (**10**)



10

Methyl (2*R*)-2-methoxymethoxypropanoate (**20**) (1.7 g, 11.9 mmol) was dissolved in diethyl ether (50 cm<sup>3</sup>) and cooled to -78 °C. DIBAL-H (1 M hexane, 26.1 cm<sup>3</sup>, 26.1 mmol) was added dropwise and the reaction mixture was allowed to attain room temperature slowly overnight. The reaction mixture was cooled to 0 °C before being quenched by the addition of a saturated solution of ammonium chloride (14 cm<sup>3</sup>) and being warmed to room temperature, giving rise to a white precipitate. The reaction mixture was filtered through a pad of Celite<sup>®</sup> and washed extensively with diethyl ether. The filtrate was then dried (MgSO<sub>4</sub>), filtered and evaporated *in vacuo*. Purification was carried out by flash column chromatography using an elution gradient of diethyl ether-petroleum ether (0%-75%) to yield (2*R*)-2-Methoxymethoxypropan-1-ol (**10**) (0.94 g, 68%) as a colourless oil.  $\nu_{\max}$  (neat)/cm<sup>-1</sup> 3558 (OH), 2933 (CH);  $[\alpha]_{\text{D}}^{15}$  -73.4 (*c* 1.0, CHCl<sub>3</sub>);  $\delta_{\text{H}}$  (400 Hz, CDCl<sub>3</sub>) 1.17 (3H, d, *J* 6.4 Hz, 3-H<sub>3</sub>), 2.95 (1H, dd, *J* 8.8, 4.0 Hz, OH), 3.42 (3H, s, OMe), 3.49 (1H, dd, *J* 7.6, 4.0 Hz, 1-HH), 3.55 (1H, dd, *J* 8.8, 2.8 Hz, 1-HH), 3.76 (2H, m, 2-H);  $\delta_{\text{C}}$  (100 MHz, CDCl<sub>3</sub>) 17.0 (CH<sub>3</sub>), 55.5 (CH<sub>3</sub>), 67.0 (CH<sub>2</sub>), 76.6 (CH), 96.1 (CH<sub>2</sub>); *m/z* (CI) 121.0867 (MH<sup>+</sup>). C<sub>5</sub>H<sub>13</sub>O<sub>3</sub> requires 121.0865).

### (2*E*,4*R*)-4-Methoxymethoxypent-2-enoate (**11**)

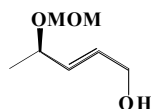


11

Methyl sulfoxide (1.32 cm<sup>3</sup>, 18.6 mmol) was added to a stirred solution of oxalyl chloride (0.82 cm<sup>3</sup>, 9.3 mmol) in dichloromethane (20 cm<sup>3</sup>) at -78 °C. This mixture was stirred for 0.25 h before (2*R*)-2-Methoxymethoxypropan-1-ol (**10**) (0.94 g, 7.75 mmol) in dichloromethane (20 cm<sup>3</sup>) was added. The mixture was stirred for a further 0.25 h before triethylamine (5.39 cm<sup>3</sup>, 38.7 mmol) was added. This reaction mixture was allowed to stir for 2 h. In a second flask, a solution of lithium chloride (0.49 g, 11.6 mmol), triethyl phosphonoacetate (2.3 cm<sup>3</sup>, 11.6 mmol) and 1,8-diazabicyclo[5.4.0]undec-7-ene (1.74 cm<sup>3</sup>, 11.6 mmol) in acetonitrile (45 cm<sup>3</sup>) was prepared and stirred for 0.5 h. The contents of the second flask were then added to the Swern solution and the reaction mixture was allowed to stir at room temperature overnight. The reaction was quenched with brine (50 cm<sup>3</sup>) and then concentrated *in vacuo*. The residue was extracted with diethyl ether (5 x 50 cm<sup>3</sup>) and the organic layers were combined, dried (MgSO<sub>4</sub>), filtered and evaporated *in vacuo*. Purification was carried out by flash column chromatography using an elution gradient of diethyl ether-petroleum ether (0%-20%) to give the *E*-allylic ester (2*E*,4*R*)-4-Methoxymethoxypent-2-enoate (**11**) (0.92 g, 63%) as a colourless oil.  $\nu_{\max}$  (neat)/cm<sup>-1</sup> 2981 (CH), 2936, 2892, 1723 (CO), 1660 (C=C), 1298;  $[\alpha]_{\text{D}}^{25}$  +85.8 (*c* 1.0, CHCl<sub>3</sub>); lit.<sup>25</sup>  $[\alpha]_{\text{D}}^{25}$  -80.0

(enantiomer,  $c$  1.0,  $\text{CHCl}_3$ );  $\delta_{\text{H}}$  (400 Hz,  $\text{CDCl}_3$ ) 1.30 (6H, m,  $\text{OCH}_2\text{CH}_3$  and 5- $\text{H}_3$ ), 3.37 (3H, s, OMe), 4.20 (2H, q,  $J$  6.8 Hz,  $\text{OCH}_2\text{CH}_3$ ), 4.35 (1H, quin of d,  $J$  6.4, 1.2 Hz, 4-H), 4.63 (2H, s,  $\text{OCH}_2\text{O}$ ), 6.00 (1H, dd,  $J$  15.6, 1.2 Hz, 2-H), 6.85 (1H, dd,  $J$  15.6, 5.6 Hz, 3-H);  $\delta_{\text{C}}$  (100 MHz,  $\text{CDCl}_3$ ) 14.2 ( $\text{CH}_3$ ), 20.5 ( $\text{CH}_3$ ), 55.4 ( $\text{CH}_3$ ), 60.4 ( $\text{CH}_2$ ), 71.0 (CH), 94.4 ( $\text{CH}_2$ ), 120.9 (CH), 148.7 (CH), 166.3 (CO);  $m/z$  (CI) 189.1129 ( $\text{MH}^+$ .  $\text{C}_9\text{H}_{17}\text{O}_4$  requires 189.1127).

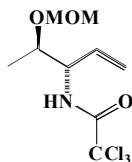
**(2E,4R)-4-Methoxymethoxypent-2-en-1-ol (12)**



12

(2E,4R)-4-Methoxymethoxypent-2-enoate (**11**) (0.87 g, 4.61 mmol) was dissolved in diethyl ether (25  $\text{cm}^3$ ) and cooled to  $-78$   $^\circ\text{C}$ . DIBAL-H (1 M hexane, 10.15  $\text{cm}^3$ , 10.15 mmol) was added dropwise and the reaction mixture was allowed to attain room temperature slowly overnight. The reaction mixture was cooled to  $0$   $^\circ\text{C}$  before being quenched by the addition of a saturated solution of ammonium chloride (14  $\text{cm}^3$ ) and being warmed to room temperature, giving rise to a white precipitate. The reaction mixture was filtered through a pad of Celite<sup>®</sup> and washed extensively with diethyl ether. The filtrate was then dried ( $\text{MgSO}_4$ ), filtered and evaporated *in vacuo*. Purification was carried out by flash column chromatography using an elution gradient of diethyl ether-petroleum ether (0%-75%) to obtain the allylic alcohol (2E,4R)-4-Methoxymethoxypent-2-en-1-ol (**12**) (0.51 g, 76%) as a yellow oil.  $\nu_{\text{max}}$  (neat)/ $\text{cm}^{-1}$  3413 (OH), 2930 (CH), 1673 (C=C);  $[\alpha]_{\text{D}}^{18} +115.4$  ( $c$  1.0,  $\text{CHCl}_3$ ); lit.<sup>25</sup>  $[\alpha]_{\text{D}}^{25} -117.9$  (enantiomer,  $c$  1.0,  $\text{CHCl}_3$ );  $\delta_{\text{H}}$  (400 Hz,  $\text{CDCl}_3$ ) 1.28 (3H, d,  $J$  6.8 Hz, 5- $\text{H}_3$ ), 1.68 (1H, s, OH), 3.38 (3H, s, OMe), 4.16 (2H, dd,  $J$  5.6, 0.8 Hz, 1- $\text{H}_2$ ), 4.22 (1H, quin,  $J$  6.8 Hz, 4-H), 4.58 (1H, d,  $J$  6.8 Hz,  $\text{OCHHO}$ ), 4.69 (1H, d,  $J$  6.8 Hz,  $\text{OCHHO}$ ), 5.64 (1H, ddt,  $J$  15.6, 7.2, 1.6 Hz, 3-H), 5.83 (1H, ddt,  $J$  15.2, 5.6, 0.4 Hz, 2-H);  $\delta_{\text{C}}$  (100 MHz,  $\text{CDCl}_3$ ) 21.3 ( $\text{CH}_3$ ), 55.2 ( $\text{CH}_3$ ), 62.9 ( $\text{CH}_2$ ), 72.0 (CH), 93.8 ( $\text{CH}_2$ ), 130.9 (CH), 132.7 (CH);  $m/z$  (CI) 129.16 ( $\text{MH}^+ - \text{H}_2\text{O}$ ), 85.11 ( $\text{MH}^+ - \text{OCH}_2\text{OCH}_3$ ).

**(3S,4R)-3-(Trichloromethylcarbonylamino)-4-(methoxymethoxy)pent-1-ene (14)**

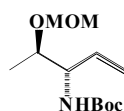


14

(2E,4R)-4-Methoxymethoxypent-2-en-1-ol (**12**) (0.45 g, 3.08 mmol) was dissolved in dichloromethane (25  $\text{cm}^3$ ) and cooled to  $0$   $^\circ\text{C}$ . 1,8-diazabicyclo[5.4.0]undec-7-ene (0.55  $\text{cm}^3$ , 3.69 mmol) and trichloroacetonitrile (0.46  $\text{cm}^3$ , 4.62 mmol) were then added and the mixture was allowed to warm to room temperature and stirred for 2 h. The reaction

mixture was then filtered through a dry silica plug and the filtrate was concentrated *in vacuo* to give an orange liquid. The crude product **13** was used without further purification. The allylic trichloroacetimidate **13** was dissolved in tetrahydrofuran (10 cm<sup>3</sup>). Bis(acetonitrile)palladium(II) chloride (0.08 g, 10% mol) was then added and the reaction mixture stirred for 24 h. Concentration *in vacuo* yielded a crude mixture of 10:1 *anti:syn* diastereomers. Purification by flash column chromatography using an elution gradient of diethyl ether-petroleum ether (0%-20%) afforded the *anti*-trichloroacetamide (3*S*,4*R*)-3-(Trichloromethylcarbonylamino)-4-(methoxymethoxy)pent-1-ene (**14**) (0.38 g, 43%) as a pale yellow oil.  $\nu_{\max}$  (neat)/cm<sup>-1</sup> 3424 (NH), 3290, 2936 (CH), 1715 (CO), 1644 (C=C), 1515, 1032;  $[\alpha]_{\text{D}}^{18}$  -56.9 (*c* 1.0, CHCl<sub>3</sub>);  $\delta_{\text{H}}$  (400 Hz, CDCl<sub>3</sub>) 1.25 (3H, *J* 6.8 Hz, 5-H<sub>3</sub>), 3.41 (3H, s, OMe), 3.84 (1H, qd, *J* 6.4, 2.4 Hz, 4-H), 4.34 (1H, m, 3-H), 4.70 (2H, q, *J* 6.8 Hz, OCH<sub>2</sub>O), 5.36 (2H, m, 1-H<sub>2</sub>), 5.88 (1H, m, 2-H), 7.93 (1H, br s, NH);  $\delta_{\text{C}}$  (100 MHz, CDCl<sub>3</sub>) 18.0 (CH<sub>3</sub>), 55.8 (CH<sub>3</sub>), 57.7 (CH), 77.05 (CH), 99.6 (CH<sub>2</sub>), 119.2 (CH<sub>2</sub>), 131.3 (CH), 161.2 (CO); *m/z* (CI) 290.0118 (MH<sup>+</sup>. C<sub>9</sub>H<sub>15</sub>Cl<sub>3</sub>NO<sub>3</sub> requires 290.0118).

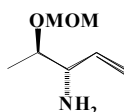
### (3*S*,4*R*)-3-(<sup>t</sup>Butyloxycarbonylamino)-4-(methoxymethoxy)pent-1-ene (**15**)



15

(3*S*,4*R*)-3-(Trichloromethylcarbonylamino)-4-(methoxymethoxy)pent-1-ene (**14**) (0.22 g, 0.76 mmol) was dissolved in a 2M solution of sodium hydroxide (40 cm<sup>3</sup>) and di-*tert*-butyl dicarbonate (0.22 g, 0.99 mmol) was added. The reaction mixture was left stirring overnight, was diluted with water (40 cm<sup>3</sup>), and was then extracted with diethyl ether (3 x 40 cm<sup>3</sup>). The organic layers were combined, dried (MgSO<sub>4</sub>), filtered and evaporated *in vacuo*. Purification was carried out by flash column chromatography using an elution gradient of diethyl ether-petroleum ether (15%-30%) to give (3*S*,4*R*)-3-(<sup>t</sup>Butyloxycarbonylamino)-4-(methoxymethoxy)pent-1-ene (**15**) (0.1 g, 55%) as a colourless oil.  $\nu_{\max}$  (neat)/cm<sup>-1</sup> 3352 (NH), 2928 (CH), 1712 (CO), 1654 (C=C), 1505, 1366, 1170;  $[\alpha]_{\text{D}}^{23}$  -61.8 (*c* 1.0, CHCl<sub>3</sub>);  $\delta_{\text{H}}$  (400 Hz, CDCl<sub>3</sub>) 1.20 (3H, d, *J* 6.4 Hz, 5-H<sub>3</sub>), 1.47 (9H, s, <sup>t</sup>Bu), 3.42 (3H, s, OMe), 3.84 (1H, q, *J* 2.8 Hz, 4-H), 4.14 (1H, m, 3-H), 4.67 (1H, d, *J* 6.8 Hz, OCHHO), 4.71 (1H, d, *J* 6.8 Hz, OCHHO), 5.27 (1H, m, 1-H<sub>2</sub>), 5.85 (1H, m, 2-H);  $\delta_{\text{C}}$  (100 MHz, CDCl<sub>3</sub>) 17.3 (CH<sub>3</sub>), 28.4 (CH<sub>3</sub>), 29.7 (CH<sub>2</sub>), 55.6 (CH<sub>3</sub>), 57.1 (CH), 76.0 (CH), 95.8 (CH<sub>2</sub>), 117.2 (CH), 134.0 (<sup>t</sup>C), 155.4 (CO); *m/z* (CI) 246.1709 (MH<sup>+</sup>. C<sub>12</sub>H<sub>24</sub>NO<sub>4</sub> requires 246.1705).

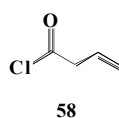
### (3*S*,4*R*)-3-Amino-4-(methoxymethoxy)pent-1-ene (**49**)



49

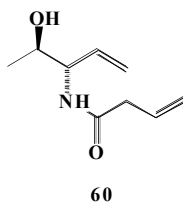
Caesium carbonate (1.6 g, 4.94 mmol) was added to a solution of (3*S*,4*R*)-3-(Trichloromethylcarbonylamino)-4-(methoxymethoxy)pent-1-ene (**14**) (0.57 g, 1.97 mmol) in acetonitrile (50 cm<sup>3</sup>). The reaction mixture was left stirring for 6 h and the solvent was evaporated *in vacuo*. The residue was partitioned between dichloromethane and water and aqueous layer was extracted. The organic layers were combined, dried (MgSO<sub>4</sub>), filtered and evaporated *in vacuo* to afford the crude amine (3*S*,4*R*)-3-Amino-4-(methoxymethoxy)pent-1-ene (**49**) (0.24 g, 83%) as a pale brown oil.  $\delta_{\text{H}}$  (400 Hz, CDCl<sub>3</sub>) 1.20 (3H, d, *J* 6.4 Hz, 5-H<sub>3</sub>), 1.60 (1H, br s, NH<sub>2</sub>), 3.40 (3H, s, OMe), 3.82 (1H, qd, *J* 6.4, 2.8 Hz, 4-H), 4.32 (1H, m, 3-H), 4.68 (1H, d, *J* 6.8 Hz, OCHHO), 4.70 (1H, d, *J* 6.8 Hz, OCHHO), 5.25 (2H, m, 1-H<sub>2</sub>), 5.85 (1H, m, 2-H).

### 3-Butenoyl chloride (**58**)



Vinylacetic acid (4.95 cm<sup>3</sup>, 58 mmol) was treated dropwise with thionyl chloride (6.79 cm<sup>3</sup>, 93 mmol) and the reaction mixture was left stirring at 40 °C for 3 h. The solution was then purified by fractional distillation at atmospheric pressure to yield 3-Butenoyl chloride (**58**) (3.1 g, 51%) at 99 °C as a colourless oil.  $\delta_{\text{H}}$  (400Hz, CDCl<sub>3</sub>) 3.64 (2H, dt, *J* 6.8 Hz, 1.6, 3-H<sub>2</sub>), 5.32 (2H, m, 1-H<sub>2</sub>), 5.92 (1H, m, 2-H).

### (3*S*,4*R*)-3-(3'-butenoylamino)-pent-1-en-4-ol (**60**)



3-Butenoyl chloride (**58**) (0.1 g, 1.03 mmol) was added to a solution of (3*S*,4*R*)-3-Amino-4-(methoxymethoxy)pent-1-ene (**49**) (0.1 g, 0.69 mmol) in dichloromethane (10 cm<sup>3</sup>). This mixture was left stirring for 0.5 h before triethylamine (0.096 cm<sup>3</sup>, 1.03 mmol) was added dropwise. The reaction mixture was left stirring overnight and was then diluted with dichloromethane (10 cm<sup>3</sup>). The organic layer was washed with 1 M hydrochloric acid solution, then with water, and finally with saturated sodium hydrogen carbonate aqueous solution, dried (MgSO<sub>4</sub>), filtered and evaporated *in vacuo*. Purification was carried out by flash column chromatography using an elution gradient of diethyl ether-petroleum ether (50-100%) and ethyl acetate (neat) to obtain (3*S*,4*R*)-3-(3'-butenoylamino)-pent-1-en-4-ol (**60**) (0.036 g, 30%) as a dark brown solid.  $\nu_{\text{max}}$  (neat)/cm<sup>-1</sup> 3326 (NH,OH), 2983 (CH), 1730(CO), 1625 (C=C).  $\delta_{\text{H}}$  (400 Hz, CDCl<sub>3</sub>, compound exists as a mixture of rotomers) 1.16 (3H, m, 5-H<sub>3</sub>, isomer A and isomer B), 1.36 (1H, s, OH), 3.01 (2H, s, 4'-H<sub>2</sub>, isomer A), 3.02 (2H, s, 4'-H<sub>2</sub>, isomer B), 3.90 (1H, m, 3-H, isomer A), 4.17 (1H, m, 3-H, isomer B), 4.41 (1H, m, 4-H, isomer A), 4.70 (1H, m, 4-H, isomer B), 4.84-5.30 (3H, m, 1-H<sub>2</sub> and 6'-H<sub>2</sub>, isomer A and isomer B), 5.71 (2H, m, 5'-H isomer A and isomer B, 4-H isomer A), 5.83 (1H, m, 4-H isomer B);

$\delta_c$  (100 MHz,  $CDCl_3$ ) 16.6 ( $CH_3$ , major isomer), 16.8 ( $CH_3$ , minor isomer), 39.2 ( $CH_2$ , major isomer), 39.3 ( $CH_2$ , minor isomer), 55.8 ( $CH$ , minor isomer), 56.2 ( $CH$ , major isomer), 73.0 ( $CH$ , major isomer), 73.3 ( $CH$ , minor isomer), 117.6 ( $CH_2$ , minor isomer), 117.7 ( $CH_2$ , major isomer), 118.7 ( $CH_2$ , major isomer), 119.1 ( $CH_2$ , minor isomer), 130.1 ( $CH$ , major isomer), 133.4 ( $CH$ , minor isomer), 134.0 ( $CH$ , major isomer), 134.7 ( $CH$ , minor isomer).

#### **4. References**

- 1) J. Mann, *Chemical Aspects Of Biosynthesis*, Oxford University Press, New York, 1994.
- 2) J. Clayden, N. Greeves, S. Warren, P. Wothers, *Organic chemistry*, Oxford University Press, New York, 2001.
- 3) T. Robinson, *The Biochemistry of Alkaloids*, Springer Verlag, New York, 1981.
- 4) P. A. Harrity, O. Provoost, *Org. Biomol. Chem.*, 2005, **3**, 1349.
- 5) P. M. Weintraub, J. S. Sabol, J. M. Kane, D. R. Borcharding, *Tetrahedron*, 2003, **59**, 2953.
- 6) P. S. Watson, B. Jiang, B. Scott, *Org. Lett.*, 2000, **2**, 3679.
- 7) G. B. Fodor, B. Colasanti, *Alkaloids: Chemical and Biological Perspectives Vol. 3*, Wiley, New York, 1985.
- 8) L. Mikhailova, *Izv. Mikrobiol. Inst.*, 1970, **21**, 291.
- 9) Y. Q. Pei, *Epilepsia*, 1983, **24**, 177.
- 10) A. Kolliker, *Arch. Path. Anat.*, 1856, **10**, 235.
- 11) D. M. R. Culbreth, *A Manual of Materia Medica and Therapeutics*, Lea & Febiger, Philadelphia/New York, 1917
- 12) W. C. Bowman, I. S. Sanghvi, *J. Pharm. Pharmacol.*, 1963, **15**, 1.
- 13) E. Leete, J. O. Olson, *J. Am. Chem. Soc.*, 1972, **94**, 5472.
- 14) B. Franck, *Chem. Ber.*, 1958, **91**, 2803.
- 15) W. T. Salter, *A Textbook of Pharmacology*, Saunders, Philadelphia/London, 1952.
- 16) R. B. Koch, D. Desaiyah, D. Foster, K. Ahmed, *Biochem. Pharmacol.*, 1977, **26**, 983.
- 17) K. Mothes, H.R. Schütte, M. Luckner, *Biochemistry Of Alkaloids*, VCH, DDR, 1985.
- 18) T. Wertheim, *Liebigs. Ann. Chem.*, 1856, **100**, 380.
- 19) M. Hesse, *Alkaloid chemistry*, Wiley, New York, 1981.
- 20) L. Marion, *The Alkaloids Chemistry and Physiology*, Academic Press Publishers, New York, 1950.

- 21) M. Scholtz, P. Pawlicki, *Chem. Ber.*, 1905, **38**, 1289.
- 22) K. W. Bentley, *The Alkaloids*, Wiley, New York, 1996.
- 23) W. F. von Öttingen, *The Therapeutic Agents of the Pyrrole and Pyridine Group*, Edwards Brothers, Michigan, 1936.
- 24) D. Elbein, R. J. Molyneux, *Alkaloids: Chemical and Biological Perspectives Vol. 5*, Wiley, New York, 1987.
- 25) K. N. Fanning, A. G. Jamieson, A. Sutherland, *Org. Biomol. Chem.*, 2005, **3**, 3749.
- 26) C. E. Anderson, L. E. Overman, M. P. Watson, *Org. Syn.*, 2005, **82**, 134.
- 27) L. E. Overman, *Acc. Chem. Res.*, 1980, **13**, 218.
- 28) T. G. Schenck, B. Bosnich, *J. Am. Chem. Soc.*, 1985, **107**, 2058.
- 29) A. G. Jamieson, A. Sutherland, *Org. Biomol. Chem.*, 2005, **3**, 735.
- 30) T. J. Donhoe, K. Blades, P. R. Moore, M. J. Waring, J. J. G. Winter, M. Helliwell, N. J. Newcombe, G. Stemp, *J. Org. Chem.*, 2002, **67**, 7946.
- 31) Y. Graillet, A. Guy, *Tetrahedron Lett.*, 1990, **50**, 7315.
- 32) S. Kim, T. Lee, E. Lee, J. Lee, G. Fan, S. K. Lee, D. Kim, *J. Org. Chem.*, 2004, **69**, 3144.
- 33) A. Padwa, M. A. Brodney, B. Liu, K. Satake, T. Wu, *J. Org. Chem.*, 1999, **64**, 3595.
- 34) D. Urabe, K. Sugino, T. Nishikawa, M. Isobe, *Tetrahedron Lett.*, 2004, **45**, 9405.
- 35) H. Takahata, Y. Banba, H. Ouchi, H. Remoto, A. Kato, I. Adachi, *J. Org. Chem.*, 2003, **68**, 3603.
- 36) R. G. Arrayás, A. Alcudia, L. S. Liebeskind, *Org. Lett.*, 2001, **21**, 3381.
- 37) S. Hanessian, H. Sailes, A. Munro, E. Therrien, *J. Org. Chem.*, 2003, **68**, 7219.
- 38) T. M. Trnka, R. H. Grubbs, *Acc. Chem. Res.*, 2001, **34**, 18.
- 39) G. Bhalay, S. Clough, L. McClaren, A. Sutherland, C. L. Willis, *Perkin Trans. I*, 2000, **6**, 901.

## Appendix

As further evidence for product ratios of the Horner-Wadsworth-Emmons reaction and the aza-Claisen rearrangement two proton nuclear magnetic resonance integration ratios are presented.

The first ratio shows the relative proportion of *E* to *Z* isomers in the outcome of the Horner-Wadsworth-Emmons reaction. The olefinic proton at the 2-position was taken as reference to suggest a 53:1 *E:Z* product ratio.

The last spectrum illustrates the ratio of *anti* to *syn* products obtained for the aza-Claisen rearrangement, in particular at the 20 h reaction time mark. The 7-methyl signal was utilised as reference for the ratio.